LUND UNIVERSITY

Precipitating Amine Absorption Systems for Carbon Capture

Karlsson, Hanna

2021

Document Version:
Publisher's PDF, also known as Version of record

Link to publication

Citation for published version (APA):
Karlsson, H. (2021). *Precipitating Amine Absorption Systems for Carbon Capture*. Chemical Engineering, Lund University.

Total number of authors:
1

General rights
Unless other specific re-use rights are stated the following general rights apply:
Copyright and moral rights for the publications made accessible in the public portal are retained by the authors and/or other copyright owners and it is a condition of accessing publications that users recognise and abide by the legal requirements associated with these rights.
• Users may download and print one copy of any publication from the public portal for the purpose of private study or research.
• You may not further distribute the material or use it for any profit-making activity or commercial gain
• You may freely distribute the URL identifying the publication in the public portal

Read more about Creative commons licenses: https://creativecommons.org/licenses/

Take down policy
If you believe that this document breaches copyright please contact us providing details, and we will remove access to the work immediately and investigate your claim.

LUND UNIVERSITY

PO Box 117
221 00 Lund
+46 46-222 00 00

Precipitating Amine Absorption Systems for Carbon Capture

HANNA KARLSSON | CHEMICAL ENGINEERING | LUND UNIVERSITY

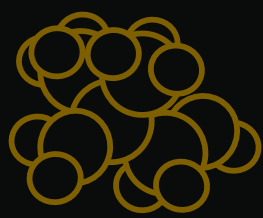

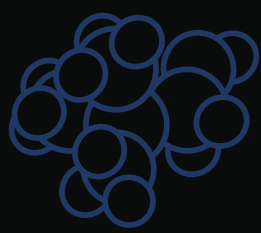

Printed by Media-Tryck, Lund 2021 NORDIC SWAN ECOLABEL 3041 0903

LUND UNIVERSITY

ISBN: 978-91-7422-838-0

Chemical Engineering
Faculty of Engineering
Lund University

Precipitating Amine Absorption Systems for Carbon Capture

Hanna Karlsson

LUND
UNIVERSITY

DOCTORAL DISSERTATION

by due permission of the Faculty of Engineering, Lund University, Sweden.
To be defended in lecture hall KC:B at the Centre for Chemistry and Chemical Engineering, Naturvetarvägen 14, Lund, on the 12th of November at 9:00.

Faculty opponent
Professor Hanna Knuutila, Department of Chemical Engineering,
Norwegian University of Science and Technology

Organization LUND UNIVERSITY Department of Chemical Engineering P.O. Box 124 SE-221 00 Lund Sweden	**Document name** DOCTORAL THESIS **Date of issue** 12th November, 2021
Author(s) Hanna Karlsson	Sponsoring organization Swedish Energy Agency, Göteborg Energi, MISTRA

Title and subtitle
Precipitating Amine Absorption Systems for Carbon Capture

Abstract

Carbon capture using amine-based absorption is an established technology for the separation of gaseous CO_2. It is used in the upgrading of gaseous fuels, and it has also been suggested that it could play a crucial role in the mitigation of climate change through post-combustion carbon capture and sequestration (CCS), and by creating carbon sinks through bioenergy CCS. One drawback of the existing technology is the high energy require¬ment associated with the regeneration of conventional aqueous amine solutions, which must be addressed in order to make amine absorption a viable option for carbon capture in the industrial sector.

The work presented in this thesis focuses on amine solutions where a sterically hindered primary amine (AMP) was studied in mixtures with organic solvents as possible alternatives to conventional aqueous amine solutions. The reason for replacing the water component is the potential reduction in temperature and energy requirement in the regeneration step. The solubility of CO_2 and heat of absorption were studied using reaction calorimetry, the chemical species in solution were characterized using nuclear magnetic resonance, and the absorption rate was studied using a wetted wall column.

The results showed that AMP in non-aqueous solutions with NMP or DMSO can be regenerated at lower temperatures (<90 °C) than with conventional aqueous amine solutions (≥120 °C). During absorption, precipitation of the AMP carbamate allowed more CO_2 to be absorbed in the solution, and precipitation was promoted by increasing the AMP concentration. However, precipitation resulted in a higher heat of absorption than for non-precipitating solutions, which adds to the overall cooling demand of the capture process. When absorption was per¬formed at 40 °C, a CO_2 partial pressure of 20 kPa was needed to obtain a similar cyclic capacity to that in 30 wt% MEA, indicating that the studied non-aqueous AMP solutions were suitable for biogas upgrading and industrial carbon capture applications. The less toxic properties of DMSO, and the overall slightly higher solubility of CO_2 in AMP/DMSO than in AMP/NMP, suggest that further studies should be carried out using 25 wt% AMP in DMSO.

The influence of water accumulation in AMP/DMSO was also studied, due to the hygroscopic properties of DMSO. It was found that the formation of bicarbonate increased with increasing water content. However, some water accumulation may not be problematic as the capacity of the absorption solutions was not reduced in the temperature range studied (40-88 °C) in solutions with a water:AMP molar ratio of 2:1. Preliminary results also indicated that water accumulation could lead to higher AMP degrad¬ation rates, but further studies are required to investigate this.

Key words
CO_2 capture, non-aqueous, AMP, solubility, heat of absorption

Classification system and/or index terms (if any)

Supplementary bibliographical information	**Language** English
ISBN (print) 978-91-7422-838-0	**ISBN (pdf)** 978-91-7422-839-7
Recipient's notes	**Number of pages** 158 Price
	Security classification

I, the undersigned, being the copyright owner of the abstract of the above-mentioned dissertation, hereby grant to all reference sources permission to publish and disseminate the abstract of the above-mentioned dissertation.

Signature 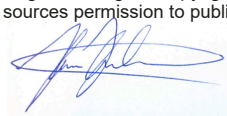 Date 2021-10-04

Precipitating Amine Absorption Systems for Carbon Capture

Hanna Karlsson

LUND
UNIVERSITY

Cover illustration by Hanna Karlsson

Copyright Introductory summary Hanna Karlsson

Paper 1 © Elsevier

Paper 2 © Elsevier

Paper 3 © Elsevier

Paper 4 © Elsevier

Paper 5 © by the Authors (Manuscript unpublished)

Faculty of Engineering
Department of Chemical Engineering

ISBN 978-91-7422-838-0 (print)
ISBN 978-91-7422-839-7 (pdf)

Printed in Sweden by Media-Tryck, Lund University
Lund 2021

Media-Tryck is a Nordic Swan Ecolabel certified provider of printed material. Read more about our environmental work at www.mediatryck.lu.se

MADE IN SWEDEN

To whom it may concern

Abstract

Carbon capture using amine-based absorption is an established technology for the separation of gaseous CO_2. It is used in the upgrading of gaseous fuels, and it has also been suggested that it could play a crucial role in the mitigation of climate change through post-combustion carbon capture and sequestration (CCS), and by creating carbon sinks through bioenergy CCS. One drawback of the existing technology is the high energy requirement associated with the regeneration of conventional aqueous amine solutions, which must be addressed in order to make amine absorption a viable option for carbon capture in the industrial sector.

The work presented in this thesis focuses on amine solutions where a sterically hindered primary amine (AMP) was studied in mixtures with organic solvents as possible alternatives to conventional aqueous amine solutions. The reason for replacing the water component is the potential reduction in temperature and energy requirement in the regeneration step. The solubility of CO_2 and heat of absorption were studied using reaction calorimetry, the chemical species in solution were characterized using nuclear magnetic resonance, and the absorption rate was studied using a wetted wall column.

The results showed that AMP in non-aqueous solutions with NMP or DMSO can be regenerated at lower temperatures (<90 °C) than with conventional aqueous amine solutions (≥120 °C). During absorption, precipitation of the AMP carbamate allowed more CO_2 to be absorbed in the solution, and precipitation was promoted by increasing the AMP concentration. However, precipitation resulted in a higher heat of absorption than for non-precipitating solutions, which adds to the overall cooling demand of the capture process. When absorption was performed at 40 °C, a CO_2 partial pressure of 20 kPa was needed to obtain a similar cyclic capacity to that in 30 wt% MEA, indicating that the studied non-aqueous AMP solutions were suitable for biogas upgrading and industrial carbon capture applications. The less toxic properties of DMSO, and the overall slightly higher solubility of CO_2 in AMP/DMSO than in AMP/NMP, suggest that further studies should be carried out using 25 wt% AMP in DMSO.

The influence of water accumulation in AMP/DMSO was also studied, due to the hygroscopic properties of DMSO. It was found that the formation of bicarbonate increased with increasing water content. However, some water accumulation may not be problematic as the capacity of the absorption solutions was not reduced in the temperature range studied (40-88 °C) in solutions with a water:AMP molar ratio of 2:1. Preliminary results also indicated that water accumulation could lead to higher AMP degradation rates, but further studies are required to investigate this.

Populärvetenskaplig sammanfattning

I takt med att vi förbränner fossila bränslen, ökar koldioxidhalten i atmosfären. Idag råder det vetenskaplig konsensus kring det faktum att den atmosfäriska koldioxidhalten är direkt kopplad till den globala medeltemperaturen, där högre halter bidrar till högre medeltemperatur. För att minimera bidraget orsakat av människor, behöver utsläppen av koldioxid drastiskt minska. Det finns olika tillvägagångsätt för att uppnå detta. Denna avhandling beskriver mitt arbete kring utveckling av ny teknik som kan användas vid produktion av biobränslen och även för att minska utsläppen av koldioxid genom koldioxidinfångning. Tekniken är baserad på vattenfria absorptionssystem i vilka koldioxid löser sig och reagerar och på så sätt separeras från olika gasblandningar.

Användandet av fossila bränslen, så som kol, olja och naturgas, är en av de största bidragande faktorerna till utsläpp av koldioxid. Att byta till biobränslen är en metod som kan användas för att minska utsläppens påverkan på koldioxidhalten i atmosfären. Detta beror på att kolet som finns bundet i biobränslen har tagits från atmosfären istället för att ha varit lagrat i bunden form under en längre tid, som i fossila bränslen. Koldioxiden som bildas vid förbränning bidrar då inte till en ökning av koldioxidhalten i atmosfären i samma utsträckning som fossila bränslen. Biogas är ett biobränsle som kan produceras vid nedbrytning av olika råvaror, t.ex. matrester och grödor, med hjälp av specifika mikroorganismer. Vid nedbrytningen av råvarorna producerar mikroorganismerna mestadels metangas och koldioxid. Eftersom koldioxid är en slutprodukt vid förbränning kommer höga halter av koldioxid påverka biogasens förmåga att fungera som ett effektivt bränsle. För att kunna använda den producerade biogasen som fordonsbränsle, eller som ersättning för naturgas, behöver man alltså ta bort koldioxiden från gasblandningen. Detta kallas för uppgradering av biogas till biometan.

För detta ändamål använder man metoder för så kallad koldioxidinfångning, inom vilka aminabsorption är en av de mest lovande teknikerna. Aminer är organiska föreningar med en kvävegrupp som reagerar med koldioxid. Detta gör aminerna lämpliga för koldioxidavskiljning eftersom de inte reagerar med övriga gaskomponenter. I kommersiella sammanhang är aminerna ofta lösta i vatten. Koldioxiden som fångas in skulle sedan kunna lagras geologiskt för att undvika att åter släppas ut i atmosfären, så kallad ”Bio-Energy Carbon Capture and Storage” (BECCS). På så sätt skulle man kunna uppnå negativa utsläpp, där koldioxid tas upp från atmosfären för att sedan inte släppas ut igen.

Vattenbaserade aminsystem är dock kopplade till ett högt energibehov för infångningsprocessen. Det stora energibehovet beror framförallt på att en stor mängd vätska måste värmas till temperaturer över 120 °C. Vid dessa temperaturer

kommer dessutom vatten att förångas i systemet vilket kräver ännu mer energi. I mitt arbete har jag undersökt vattenfria aminsystem som ett alternativ, där vattnet är utbytt mot organiska lösningsmedel. I denna typ av system reagerar aminen med koldioxid och bildar ett salt. När tillräckligt mycket koldioxid reagerat faller saltet ut som fasta kristaller i lösningen. Eftersom koldioxiden som löst sig är en del av de bildade saltkristallerna, skapar detta en möjlighet att separera de fasta partiklarna från resterande vätska. Då kan man minska mängden vätska som behöver värmas upp i processen och därmed mängden värme som behöver tillföras.

Den amin som används i studierna som täcks i denna avhandling heter 2-amino-2-metyl-1-propanol och förkortas AMP. AMP har en amingrupp som sitter längst ut på kolkedjan som utgör stommen av molekylen och bredvid den sitter två metyl-grupper. När amingruppen reagerar med koldioxid, bidrar metyl-grupperna till att rörligheten i den bildade produkten är begränsad. Detta kallas att produkten är steriskt hindrad. Steriskt hindrade reaktionsprodukter är mindre stabila, vilket leder till att det inte krävs lika höga temperaturer för regenerering, jämfört med system där produkterna som bildas är mer stabila. För de lösningar som studerats i denna avhandling kan man återfå merparten av koldioxiden i gasfas vid 70-90 °C, vilket betyder att man skulle kunna använda överskottsvärme för att driva processen istället för energi av högre kvalitet.

Jag har studerat AMP i kombination med olika lösningsmedel, exempelvis N-metyl-2-pyrrolidon och dimetylsulfoxid, och utvärderat om dessa skulle lämpa sig för koldioxidavskiljning. Bland annat har jag undersökt hur mycket koldioxid som kan lösa sig i aminlösningen vid olika temperaturer, för att få en uppfattning om hur mycket koldioxid som kommer finnas i vätskan under absorptionen samt vid regenereringen. Skillnaden däremellan kallas den cykliska kapaciteten och ger en uppskattning av hur mycket aminlösning som kommer behövas för att fånga en specifik mängd koldioxid. Resultaten från mitt arbete visar att den cykliska kapaciteten är jämförbar med kommersiella vattenbaserade aminsystem samt att lösningarna lämpar sig bäst för koldioxidavskiljning vid biogasuppgradering och i industrin, där man ofta har lite högre halter av koldioxid i gasen som ska renas.

Vattenfria system med AMP är intressanta eftersom huvuddelen av koldioxiden kan fångas i fasta kristallpartiklar som kan avskiljas från lösningsmedlet och eftersom det går att reversera reaktionen mellan koldioxid och AMP vid lägre temperaturer än många andra aminbaserade system. Eftersom lägre temperaturer kan användas, samtidigt som de organiska lösningsmedlen har högre kokpunkt än vatten, innebär det också att mindre förångning sker under regenereringen. Sammanlagt bidrar detta till en mer energieffektiv process för koldioxidinfångning än de som är kommersiellt tillgängliga idag.

List of Publications

I. **Karlsson, H.K.**, Sanku, M., Svensson, H., Absorption of carbon dioxide in mixtures of N-methyl-2-pyrrolidone and 2-amino-2-methyl-1-propanol, *International Journal of Greenhouse Gas Control*, 2020, vol. 95, 102952

II. **Karlsson, H.K.**, Drabo, P., Svensson, H., Precipitating non-aqueous amine systems for absorption of carbon dioxide using 2-amino-2-methyl-1-propanol, *International Journal of Greenhouse Gas Control*, 2019, vol. 88, pp. 460-468

III. **Karlsson, H.K.**, Makhool, H., Karlsson, M., Svensson, H., Chemical absorption of carbon dioxide in non-aqueous systems using the amine 2-amino-2-methyl-1-propanol in dimethyl sulfoxide and N-methyl-2-pyrrolidone, *Separation and Purification Technology*, 2021, vol. 256, 117789

IV. **Karlsson, H.K.**, Svensson, H., Rate of absorption for CO_2 absorption systems using a wetted wall column, *Energy Procedia*, 2017, vol. 114, pp. 2009-2023

V. **Karlsson, H.K.**, Karlsson, M., Svensson, H., Evaluation of the effect of water on CO_2 absorption in AMP and DMSO systems, *Manuscript*

The Author's Contributions

I. I planned the study together with my co-authors, and performed the amine experiments and data evaluation. I participated in the preparation of the manuscript and the final review of the article.

II. I planned the study together with my co-authors, and performed most of the experiments and data evaluation. I wrote the manuscript.

III. I planned the study together with my co-authors, and performed most of the experimental work and data evaluation. I wrote the manuscript.

IV. I participated in the planning of the experiments together with my co-author. I built the experimental setup, performed the experiments and evaluated the data. I wrote the manuscript.

V. I planned the study together with my co-authors. I performed the calorimetric experiments and evaluated the data. I wrote the manuscript together with my co-authors.

Other Related Publications

Wang, W., Sanku, M., **Karlsson, H.K.**, Hulteberg, C., Karlsson, H.T., Balfe, M., Stallmann, O., Medium temperature desulfurization for oxyfuel and regenerative calcium cycle, *Energy Procedia*, 2017, vol. 114, pp. 271-284

Karlsson, H.K., Svensson, H., Physical Properties of the 2-Amino-2-Methyl-1-Propanol and N-Methyl-2-Pyrrolidone System, *14th Greenhouse Gas Control Technologies Conference Melbourne 21-26 October 2018 (GHGT-14)*, available at SSRN: https://ssrn.com/abstract=3366000

Svensson, H., **Karlsson, H.K.,** Solubility of Carbon Dioxide in Mixtures of 2-Amino-2-Methyl-1-Propanol and N-Methyl-2-Pyrrolidone at Absorption and Desorption Conditions, *14th Greenhouse Gas Control Technologies Conference Melbourne 21-26 October 2018 (GHGT-14)*, available at SSRN: https://ssrn.com/abstract=3366169

Sanku, M., **Karlsson, H.K.**, Hulteberg, C., Wang, W., Stallmann, O., Karlsson, H.T., Kinetic evaluation of lime for medium-temperature, desulfurization in oxy-fuel conditions by dry sorbent injection, *Energies*, 2019, vol. 12, 2645-2661

Blomberg, S., Hejral, U., Shipilin, M., Albertin, S., **Karlsson, H.**, Hulteberg, C., Lömker, P., Goodwin, C., Degerman, D., Gustafson, J., Schlueter, C., Nilsson, A., Lundgren, E., Amann, P., Bridging the pressure gap in CO oxidation, *ACS Catalysis*, 2021, vol. 11, 9128-9135

Acknowledgements

I dedicate this page to all the amazing people who helped and supported me throughout my PhD years, both professionally and emotionally.

First and foremost, I would like to thank my supervisors Helena and Christian. Thank you both for pushing me out of my comfort zone and for giving me the opportunity to stay for a PhD. I have learned so much from both of you! Helena, thank you for your support and all the great scientific discussions over the years. Working with you has not only been inspiring but also really, really fun! Thank you for putting up with my insecurities and helping me to overthink things less and realize that I can do this! Christian, thank you for your child-like enthusiasm for nerdy things, which have contributed to many great and helpful discussions. It has been both inspiring and helpful!

Endless thanks to my present and former colleagues in the Innovative process design research group, who all have contributed to my many "AHA!" experiences during the years. Special thanks to Meher Geetika, who always found time for great and well-needed discussions, both work related and personal. Thank you Sara, for allowing me to participate in your synchrotron activities, they have been both super fun and great learning experiences! Thank you Per for all the time you spent with me in the lab, helping me with my first setup and teaching me how to Swagelok! To my great office mate Kena, thank you for all the good times (and all the good food), I told you we would finish! Thank you Laura for the everyday craziness and awesome adventures.

Then I would like to thank all the fantastic people at the department of Chemical Engineering, for making everyday fun and sometimes a little crazy! Micke, thank you for the philosophical discussions of, not only research, but also life, the universe and everything! Henrik, thank you for the coffee break therapy sessions and for great discussions on cleaning. Special thanks also to Herje and Mats, you are both such optimistic and happy people and every discussion with you has been a delight! Thanks to Maria and Gity for helping me with paperwork and administrative things, and to Bori for making sure I got the chemicals I needed.

I would also like to thank all my family and friends for their emotional support throughout this process. You are great cheerleaders! Special thanks to Mamma and Sabrina for keeping me mentally sane, and to Pappa for the great discussions and fun collaboration (I guess I was nerdy enough for a PhD after all)!

Last but not least, I would like to thank all the tired, involuntary members of the procrastinating academics support group (you know who you are). Hang in there, you can do it! (*if not today, then tomorrow*)

Abbreviations and Symbols

Abbreviations

10A-D	10 wt% AMP in DMSO
10A-D4W	10 wt% AMP and 4 wt% water in DMSO
15A-N	15 wt% AMP in NMP
1P	1-Pentanol
23A-D9W	23 wt% AMP and 9 wt% water in DMSO
24A-D5W	24 wt% AMP and 5 wt% water in DMSO
25A-1P	25 wt% AMP in 1-P
25A-4H	25 wt% AMP in 4-heptanone
25A-D	25 wt% AMP in DMSO
25A-DMAPN	25 wt% AMP in DMAPN
25A-N	25 wt% AMP in NMP
25A-T	25 wt% AMP in TEGDME
30A-N	30 wt% AMP in NMP
30M-W	30 wt% MEA in water

AMP	2-Amino-2-methyl-1-propanol
BECCS	Bioenergy carbon capture and sequestration
CCS	Carbon capture and sequestration
^{13}C NMR	Carbon-13 nuclear magnetic resonance
DEGMME	diethylene glycol monomethyl ether
DMAPN	3-Dimethylaminopropionitrile
DMOZD	4,4-dimethyl-1,3-oxazolidin-2-one
DMSO	Dimethyl sulfoxide
EG	Ethylene glycol
IPCC	Intergovernmental Panel on Climate Change

LVC	Lean vapor compression
MEA	Monoethanolamine
MFC	Mass flow controller
NAS	Non-aqueous solvent
NMP	N-methyl-2-pyrrolidone
PFO	Pseudo-first-order
PZ	Piperazine
SOC	Stripper overhead compression
TEGDME	Triethylene glycol dimethyl ether
VLE	Vapor–liquid equilibrium
WLS	Water-lean solvent
WWC	Wetted wall column

Symbols

C	Concentration	[mol/m^3]
D	diffusivity	[m^2/s]
E	Enhancement factor	[-]
Ha	Hatta number	[-]
H_{CO2}	Henry's constant	[Pa·m^3/mol]
k'_g	Liquid-side mass transfer coefficient	[mol/(m^2·s·Pa)]
k_2	Second-order rate constant	[m^3/(s·mol)]
k_g	Gas-side mass transfer coefficient	[mol/(m^2·s·Pa)]
K_G	Overall mass transfer coefficient	[mol/(m^2·s·Pa)]
k_l	Liquid-side mass transfer coefficient	[m/s]
k_l^0	Physical mass transfer coefficient	[m/s]
m	Molal, concentration	[mol/kg]
M	Molar, concentration	[mol/dm^3]
n	molar amount	[mol]
N_{CO2}	CO_2 flux	[mol /(m^2·s)]

P	Pressure	[Pa]
Q	heat production	[J]
R	molar gas constant	[J/(mol·K)]
T	Temperature	[K]
V	volume	[m^3]
x	Mole fraction	[-]
α	Loading	[mol CO_2/mol AMP]
ΔH	Change in enthalpy	[J/mol]
ν	stoichiometric ratio	[-]

Subscripts

0	Initial
∞	Infinite
abs	Absorbed
g	Gas
i	interface
lq	Liquid
Phase	Phase-change
Reg	Regeneration
Rxn	Reaction
s	Solid
Sens	Sensible
sol	Soluted
vap	Vaporization

Contents

1 Introduction

The extensive and increasing use of fossil fuels since the end of the 19th century has led to a rapid increase in greenhouse gas emissions. CO_2 alone accounts for almost three-quarters of the annual global emissions (Ritchie and Roser, 2020), which has led to an increase in atmospheric CO_2 levels. In 2020, the yearly mean atmospheric CO_2 concentration was 412 ppm (Dlugokencky and Tans, 2021), compared to pre-industrial levels of around 280 ppm (Butler, 2013). In order to minimize the impact on the climate resulting from these emissions, much research in modern times has focused on ways of reducing our dependence on fossil fuels and reducing emissions of anthropogenic CO_2. Switching to renewable energy sources is an essential step towards this goal.

However, the rate at which renewable biofuels are being introduced is relatively slow, especially bearing in mind the growing global energy demand. In 2019, 84% of the global primary energy consumption was based on fossil fuels (Ritchie, 2020). The aim set in the Paris Agreement of 2015 was to limit the increase in global temperature in the 21th century to below 2 °C (preferably a maximum increase of 1.5 °C), compared to pre-industrial times (United Nations Framework Convention on Climate Change, 2015). However, global CO_2 emissions continue to increase due to rising energy demands. The temporary decrease in CO_2 emissions of 5.8% observed during 2020 as a consequence of the COVID-19 pandemic (IEA, 2021), gives an indication of the extensive measures that needs to be taken to reduce CO_2 emissions without implementation of CO_2 reduction technologies. This suggests that CO_2 reduction technologies, such as carbon capture and sequestration (CCS) will be necessary if we are to achieve drastic reductions of the global CO_2 emissions and reach the climate goals.

The Intergovernmental Panel on Climate Change (IPCC) published a special report in 2018 on the impacts of a 1.5 °C increase in global temperature, including various means of achieving this target (Rogelj et al., 2018). In most of the IPCC scenarios, CO_2 reduction technologies resulting in negative emissions are required in order to limit the global temperature increase to 1.5 °C. Bioenergy with carbon capture and sequestration (BECCS) is therefore predicted to play an important role in the mitigation of climate change. One possible way of implementing BECCS could be to store the CO_2 that is removed in the upgrading of gaseous biofuels, such as biogas.

The work presented in this thesis is focused on carbon capture techniques using novel CO_2 absorption systems. These systems, employing non-aqueous precipitating amine solutions, were evaluated regarding their potential to capture CO_2 from both biogas (i.e., biogas upgrading) and industrial flue gases (i.e., post-combustion carbon capture). The rest of this chapter provides a brief introduction to the work. The capture of CO_2 from gas streams is described in Section 1.1, together with the two main applications, biogas upgrading and post-combustion carbon capture. The research questions addressed and the overall aim of this work are presented in Section 1.2, followed by the outline of the thesis in Section 1.3.

1.1 CO_2 capture from gaseous mixtures

Biogas is an example of a renewable fuel that can be produced from organic matter. It is mainly produced by the bacterial conversion of biomass through anaerobic digestion. The constituents of the resulting biogas are mainly methane (CH_4) and CO_2, but minor amounts of impurities such as water vapor, hydrogen, nitrogen, carbon monoxide and hydrogen sulfide can also be present (Deng et al., 2020). Various kinds of feedstocks can be used in the production of biogas, e.g., agricultural and industrial feedstocks, municipal waste and aquatic biomass (Al Seadi et al., 2013). The composition of the biogas therefore varies greatly, and may contain 45-70% CH_4 and 30-55% CO_2 (Angelidaki et al., 2018).

Biogas is commonly used for the production of heat and electricity and, depending on the circumstances and equipment used, it can be burned "as is" without further purification. However, in most cases, some gas cleaning is necessary, for example, the removal of hydrogen sulfide to avoid corrosion, or particular matter to avoid fouling (Deng et al., 2020). If the biogas is to be used as a vehicle fuel, or for injection into the gas grid as a substitute for natural gas, it must be upgraded to biomethane. In the gas upgrading process, CO_2 is removed in order to obtain a gas consisting of mostly CH_4, with a higher energy density than the raw biogas. In Sweden, the required level of CH_4 for vehicle gas or injection to the gas grid is 97% (Cigni et al., 2006; Klackenberg, 2020).

In post-combustion carbon capture, CO_2 is captured and removed from flue gases after the combustion of fuels (both fossil fuels and biofuels). If the fuel is combusted with air, the main constituent is N_2 (typically over 70%), followed by water vapor and oxygen. Impurities such as SO_x, NO_x and particular matter are also present. The CO_2 content in flue gases varies depending on the application and fuel used. Typical CO_2 concentrations in power production are 10-15% for coal-fired power plants, and below 10% for natural gas turbines (Lackner et al., 2010; Song et al., 2004). The CO_2 concentration in industrial flue gases varies considerably, depending on the source. For example, the CO_2 concentration in the flue gases at the SSAB

steelworks in Luleå, northern Sweden, is around 24-30% (Skagestad et al., 2017), and at the Preem refinery in Lysekil, Sweden, 97% of the total CO_2 emissions comes from flue gases in which the CO_2 concentration ranges from 7 to 24% (Haugen et al., 2013).

Similar techniques can be used for the removal of CO_2 in both biogas upgrading and post-combustion carbon capture. Examples of techniques used are physical and chemical absorption or adsorption, and membrane separation. One of the most commonly used techniques is amine absorption, in which CO_2 is removed from the gas by reaction with an amine in a liquid solution, at relatively low temperatures and pressures. Various amine solutions can be used for this purpose, depending on the process conditions and requirements. Industrially, aqueous amine solutions using amines such as monoethanolamine (MEA), diethanolamine (DEA), N-methyl diethanolamine (MDEA) and diglycolamine (DGA) are typically used in gas upgrading (Angelidaki et al., 2019).

The compositions of biogas and flue gases differ considerably. This means that different amine solutions may be suitable for different applications. Biogas usually has a significantly higher CO_2 content than flue gases, which means that absorption will be carried out at a higher partial pressure of CO_2 in biogas upgrading. Depending on the production route and feedstock, biogas contains little or no oxygen, whereas flue gases from combustion typically contain a few percent by volume. This means that oxidative degradation is likely to be more pronounced in post-combustion carbon capture where oxygen is present. Thus, when evaluating novel amine systems, it is necessary to investigate how the system behaves under different conditions to evaluate its suitability in different applications.

1.2 Overall aim and research questions

The aim of the work described in this thesis was to evaluate the potential of precipitating non-aqueous amine absorption as a carbon capture technique. The research focused on the use of the amine 2-amino-2-methyl-1-propanol (AMP) in non-aqueous solutions with organic solvents. Various non-aqueous AMP solutions were studied to identify possible benefits of such systems and any challenges that may arise. The investigation on whether non-aqueous precipitating AMP systems are suitable for carbon capture was performed by addressing the following research questions.

RQ1. Under which absorption and regeneration conditions could different non-aqueous AMP solutions be suitable for carbon capture?

a. Which temperatures are suitable for CO_2 absorption and regeneration of non-aqueous AMP systems?

b. How does the CO_2 partial pressure affect absorption and regeneration of CO_2 in non-aqueous AMP systems?

c. How do AMP concentration and precipitation of the AMP carbamate affect the absorption of CO_2 in non-aqueous AMP systems?

d. How are the absorption and regeneration of CO_2 affected by water accumulation in non-aqueous AMP systems?

RQ2. What are the potential benefits of using non-aqueous AMP solutions compared to conventional aqueous amine systems?

The findings of this research are presented in **Papers I-V**, which are appended at the end of this thesis. **Paper I** describes the study of the solubility of CO_2 and heat of absorption in non-aqueous solutions of AMP in N-methyl-2-pyrrolidone (NMP), at temperatures up to 88 °C. The results on the rate of absorption of CO_2 in the benchmark system of aqueous MEA and non-aqueous solutions of AMP/NMP using a wetted wall column, are presented in **Paper IV**. **Paper II** describes a screening study of AMP in 7 different organic solvents at absorption conditions. One of the most promising candidates identified, AMP in dimethyl sulfoxide (DMSO), was further evaluated, as described in **Paper III**. Absorption behavior was studied in terms of solubility and heat of absorption at temperatures up to 88 °C. The chemical species in solution at absorption and regeneration temperatures was studied using ^{13}C NMR, and compared for solutions of AMP/DMSO and AMP/NMP. The study presented in **Paper V** was carried out to evaluate the influence of accumulated water on the absorption properties of CO_2 in AMP/DMSO.

1.3 Outline

The background to this work is presented in Chapter 2, where the technique of chemical CO_2 absorption using amine solutions is described. It covers the current state of the art using aqueous amine solutions, followed by the introduction of alternative amine solutions and why these are attracting interest in this field of research. Chapter 3 presents the experimental methods used to obtain the results presented in this thesis. The main results of this work on novel amine solutions for CO_2 absorption are presented in Chapter 4, followed by conclusions and suggestions for future work in Chapters 5 and 6, respectively.

2 Chemical Absorption using Amines

Amines react selectively with acidic gases such as CO_2. Amine-based absorption systems for carbon capture are often end-of-pipe technologies, where CO_2 is removed from gaseous streams, i.e., flue gases or biogas. This is a mature technology, and is considered one of the most promising for carbon capture, as it can be retro-fitted to existing industrial plants (Rochelle, 2009).

Conventional amine absorption systems employ aqueous amine solutions. One example is aqueous solutions of the alkanolamine MEA. Aqueous MEA is considered a benchmark solution in carbon capture contexts, due to extensive studies on the system over the years, and the large amount of data available in literature. Efforts to find amine absorption systems with improved properties for carbon capture, such as higher CO_2 absorption capacity or absorption rates, have led to the development of new amine solutions. A system consisting of aqueous piperazine (PZ) and AMP has recently been proposed as a new benchmark (Feron et al., 2020). However, aqueous MEA is still widely used for comparison purposes, and was thus used as the benchmark in the work presented in this thesis.

The following sections describe the basics of chemical absorption, using aqueous MEA as an example. This is followed by an introduction to alternative approaches, such as non-aqueous and phase-changing absorption systems, and the potential benefits such systems might bring.

2.1 Aqueous amine absorption

The proposed reaction mechanism for CO_2 in aqueous solutions of the primary amine MEA, involves the formation of the MEA carbamate and, since water is present, the formation of bicarbonate. The reactions involved in the case of primary amines (RNH_2) in aqueous solutions, according to the zwitterion mechanism, are given in Reactions 1-4 below (Caplow, 1968; Danckwerts, 1979; Vaidya and Kenig, 2007).

$$CO_2 + RNH_2 \leftrightarrow RNH_2^+COO^- \quad \{1\}$$

$$RNH_2^+COO^- + \mathrm{RNH_2} \leftrightarrow RNHCOO^- + \mathrm{RN}H_3^+ \quad \{2\}$$

$$RNH_2^+COO^- + H_2O \leftrightarrow HCO_3^- + RNH_3^+ \quad \{3\}$$

$$RNHCOO^- + H_2O \leftrightarrow HCO_3^- + RNH_2 \quad \{4\}$$

Water can also participate in additional reactions in aqueous solutions, according to Reactions 5-8 (Puxty and Maeder, 2016; Vaidya and Kenig, 2007).

$$RNH_2 + H_2O \leftrightarrow RNH_3^+ + OH^- \quad \{5\}$$

$$H_2O \leftrightarrow H^+ + OH^- \quad \{6\}$$

$$CO_2 + OH^- \leftrightarrow HCO_3^- \quad \{7\}$$

$$CO_2 + H_2O \leftrightarrow HCO_3^- + H^+ \quad \{8\}$$

For amines that form stable carbamates, the formation of bicarbonate (Reactions 3-4) is limited. This is the case for aqueous MEA, where the overall reaction can be written according to Reaction 9, with a maximum loading of 0.5 CO_2/mol MEA.

$$CO_2 + 2\,RNH_2 \leftrightarrow RNHCOO^- + RNH_3^+ \quad \{9\}$$

If the amine is sterically hindered, thus forming a sterically hindered carbamate in the reaction with CO_2, bicarbonate formation is favored in aqueous solutions. This is the case for the primary alkanolamine AMP, where the maximum theoretical loading of CO_2 in an aqueous system is 1 mol CO_2/mol AMP, according to Reaction 10.

$$CO_2 + RNH_2 + H_2O \leftrightarrow HCO_3^- + RNH_3^+ \quad \{10\}$$

The above equilibrium reactions take place in an absorption column, where the different CO_2-containing species are formed in the amine solution. The reactions are then reversed in a stripping column to regenerate the gaseous CO_2. A schematic of a simple CO_2 capture plant using conventional aqueous amine solutions is presented in Figure 1. The CO_2-containing gas enters at the bottom of a counter-current absorption column, where the gas comes into contact with the amine solution. The gaseous CO_2 is absorbed in the liquid, where it reacts with the amine. The solution, which is now rich in CO_2, exits at the bottom of the absorber. Before entering the stripping column, the CO_2-rich solution is pumped through a heat exchanger where it is pre-heated using the lean solution exiting the stripper. The temperature in the stripper is raised further to the regeneration temperature needed to desorb CO_2. The lean solution is then returned, through the heat exchanger, back to the absorption

column. A mixture of desorbed CO_2 and water vapor from the stripper passes through a condenser, where the water is condensed and recycled back to the stripper. If the CO_2 is to be transported in pipelines and stored geologically, it must be compressed to around 150 bar after the regeneration step (Aspelund and Jordal, 2007; Rochelle, 2009; Roussanaly et al., 2013).

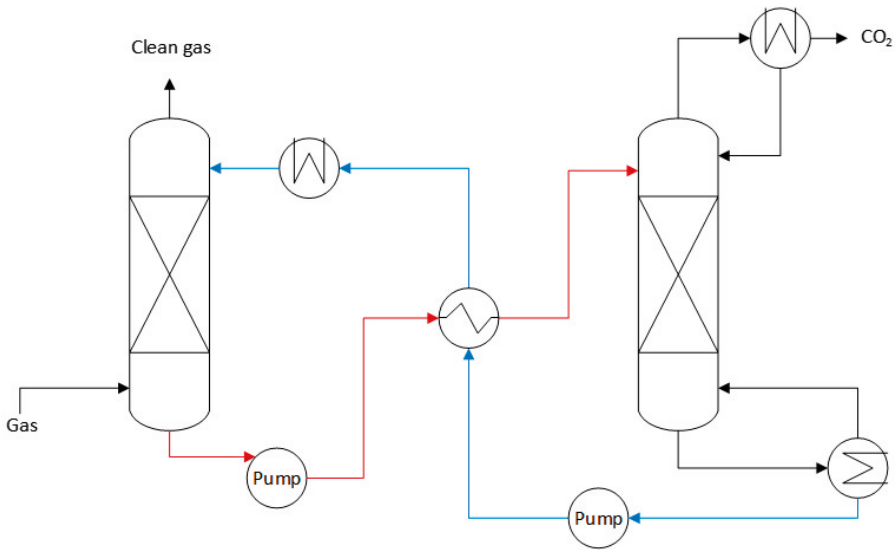

Figure 1. Schematic of a simple amine absorption process including an absorption column, stripping column and heat exchange between the CO_2-rich (red) and lean (blue) solution.

The lean amine solution and the CO_2-containing gas are typically cooled to 40 °C before entering the absorption column. Since the absorption reactions (moving to the right in Reactions 9-10) are usually exothermic, heat is evolved, causing a temperature increase in the absorption column. This increase is dependent on the heat of absorption and the heat capacity of the solution, both of which can vary between different absorption solutions. The heat of absorption (ΔH_{abs}) includes the heat of dissolution (ΔH_{sol}) as CO_2 dissolves in the absorption solution, and the heat of reaction (ΔH_{rxn}) from CO_2 reacting with the species in solution, according to Eq. 2.1.

$$\Delta H_{abs} = \Delta H_{sol} + \Delta H_{rxn} \qquad (2.1)$$

During regeneration, the equilibrium reactions must be shifted towards the desorption of CO_2. The heat required for regeneration (ΔH_{reg}) includes the heat needed to raise the temperature of the solvent to the appropriate regeneration temperature (sensible heat, ΔH_{sens}) and the heat needed to reverse the reactions taking place during the absorption of CO_2 (heat of absorption). For conventional aqueous

systems, temperatures of ≥120 °C are usually used for regeneration. In addition, the energy requirement also includes the heat of vaporization (ΔH_{vap}) for the water component. The heat of regeneration can thus be expressed according to Eq. 2.2. It should be noted that as the heat of absorption varies with temperature, its value may be different at absorption and regeneration conditions.

$$\Delta H_{reg} = \Delta \mathrm{H_{abs}} + \Delta H_{sens} + \Delta H_{vap} \qquad (2.2)$$

Literature data for the solubility of CO_2 in 30 wt% aqueous MEA at 40 and 120 °C, are shown in Figure 2 (Aronu et al., 2011a; Jou et al., 1995; Ma'mun et al., 2005; Shen and Li, 1992; Tong et al., 2012; Wanderley et al., 2020a). The partial pressure of CO_2 plays an important role during both absorption and desorption. Absorption is usually carried out at ambient pressure (Feron, 2016). The maximum rich loading, or absorption capacity, can thus be estimated from the partial pressure of CO_2 in the incoming gas. For flue gases in coal-fired power production, where the pressure corresponds to approximately 10-15 kPa, the maximum CO_2 loading is about 0.52 mol CO_2/mol MEA. For biogas, where the CO_2 content is higher, slightly higher loadings can be achieved. For a CO_2 partial pressure of 50 kPa this corresponds to about 0.6 mol CO_2/mol MEA. During regeneration, the partial pressure of CO_2 is dependent on the amount of steam that is produced in the stripper and the total pressure in the column. For aqueous MEA, lean loadings of around 0.2 are usually achieved at CO_2 partial pressures of about 10 kPa (Aronu et al., 2014; Knuutila and Nannestad, 2017). The amount of CO_2 that can be captured by a specific system, called the cyclic capacity, can be estimated from the solubility data as the difference between the rich and lean loadings under absorber and stripper conditions, respectively. In the case of 30 wt% aqueous MEA above, the cyclic capacity is typically slightly above 0.3 mol CO_2/mol MEA.

One of the major disadvantages of carbon capture is the high cost associated with the process. From a CCS perspective, over 70% of the cost is associated with capturing and compressing the CO_2 to the pressures required for geological storage (Vitillo et al., 2017). The cost must therefore be reduced to make CCS a viable option. When using aqueous MEA and the process design illustrated in Figure 1, the regeneration step, where the absorption solution is heated, has the highest energy demand, accounting for 70-80% of the operating cost (Aaron and Tsouris, 2005). The energy consumption of commercial CO_2 capture plants using aqueous MEA is in the range 3.5-4.3 GJ/ton CO_2 (Arachchige and Melaaen, 2013).

Figure 2. Literature data for CO_2 solubility in 30 wt% aqueous MEA presented as CO_2 partial pressure (P_{CO2}) as a function of loading (α), at 40 °C (green) (Aronu et al., 2011a; Jou et al., 1995; Shen and Li, 1992; Tong et al., 2012; Wanderley et al., 2020a) and 120 °C (orange) (Jou et al., 1995; Ma'mun et al., 2005; Tong et al., 2012; Wanderley et al., 2020a).

One way of reducing the energy required for regeneration, and thus the operating cost, is to introduce advanced process configurations. This is usually done in order to improve the absorption or thermal integration (Le Moullec and Neveux, 2016). Although the temperature required for regeneration is the same, increasing the cyclic capacity of the absorption solution decreases the solvent flow rate, which may reduce the energy requirement. Examples of absorption enhancement are intercooling of the solution in the absorption step to lower the temperature of the absorption solution and thus achieve higher rich loadings, and recirculating the rich solution at the bottom of the absorber to achieve longer contact times and thus higher rich loadings. The aim of thermal integration is better heat recovery within the capture process, for example, minimizing waste heat and utilizing the heat in the different process streams. There are many examples of advanced stripper configurations, two of which are stripper overhead compression (SOC) and lean vapor compression (LVC) (Le Moullec and Neveux, 2016). In SOC, the gas exiting at the top of the stripper is compressed and then condensed to release heat, which can be used to pre-heat the rich solution (Oh et al., 2020) or be used in the stripper reboiler. In LVC, the hot lean solution exiting the stripper is flashed to obtain a gaseous stream (mostly CO_2 and H_2O) that can be compressed and reintroduced into the stripper at a higher temperature, thus reducing the reboiler duty. Knudsen et al. reported a 20% decrease in reboiler duty for 30 wt% aqueous MEA when LVC was

implemented in a pilot plant (Knudsen et al., 2011). Using simulations, Oh et al. found that stripper configurations employing combined SOC and LVC for regeneration of 30 wt% aqueous MEA reduced the reboiler duty by almost one third (Oh et al., 2020). However, the potential benefit of implementing both SOC and LVC must be evaluated for individual cases due to the extra electricity required for compression. Another type of configuration is the advanced flash stripper, in which the normal stripper reboiler is replaced with a steam heater and flash vessel (Lin and Rochelle, 2016; Rochelle, 2016). Several heat exchangers are used to recover heat from the gas and the hot lean solution leaving the stripper, as well as from the water from the flash vessel. Advanced flash stripping has been tested successfully on pilot scale using aqueous PZ, and was found to reduce the heat duty by over 25% compared to previous stripper designs (Lin et al., 2016).

Although changing the stripper configuration has shown considerable potential in reducing the energy required by aqueous amine systems, there has been a simultaneous increase in interest in alternative absorption solutions, also with the aim of reducing the energy requirement, and thus the cost of carbon capture. Examples of such systems are water-lean and non-aqueous systems, where the water component in the absorption solution is replaced with organic solvents, in order to reduce the sensible heat and heat of vaporization compared with aqueous systems. Interest has also been shown in alternative absorption solutions showing phase changing behavior, either phase-splitting liquids or precipitating systems. These systems employ unconventional capture design, where less solution has to be regenerated, potentially reducing the energy requirement. These alternative types of absorption systems are discussed in the following sections.

2.2 Water-lean and non-aqueous absorption systems

Replacing water in the absorption solution with an organic solvent, or solvent mixture, is one approach in trying to reducing the energy required for carbon capture, while still using a process design and infrastructure similar to those in conventional aqueous systems. These types of systems are referred to as a water-lean solvent (WLS) when some of the water is replaced, and a non-aqueous solvent (NAS) when all the water is replaced.

Many different types of absorption solutions are classified as WLSs or NASs. Examples are non-aqueous amine blends, amino silicones, switchable carbamates, ionic liquids, amino acids in organic solvents, alkyl carbonates, N-heterocyclic azoles and hybrid systems (combinations of organic and inorganic components) (Heldebrant et al., 2017). However, this section focuses on absorption solutions based on amines and organic solvents.

The addition of an organic solvent to an absorption solution alters the physical properties of the system. The heat of vaporization can be reduced by choosing a solvent that is less volatile and has a higher boiling point than water, which reduces the amount of solvent that evaporates during regeneration. Solvents with specific heat capacities lower than that of water can also reduce the amount of energy needed to heat the solution before entering the regeneration column, thus lowering the sensible heat needed for regeneration. In addition, organic solvents can provide higher solubility of CO_2 than water, increasing the mass transfer in the absorption step, potentially leading to higher absorption rates (Wanderley et al., 2019).

As many organic solvents are hygroscopic, water can accumulate in a NAS if the incoming gas is humid. This may change the properties of the absorption system, as the presence of water enables the formation of other species in solution according to Reactions 5-8. The distribution of reaction products will thus change with the accumulation of water in the absorption system. This may result in the need to dry the incoming gas, or remove water from the absorption solution. Some water in the system can, however, be beneficial at the absorption stage, due to its high heat of vaporization (Wanderley and Knuutila, 2020). In aqueous absorption systems, some water is evaporated in the absorption column by the heat evolved by the exothermic reactions taking place, which reduces the increase in temperature of the solution. In a NAS where less evaporation occurs during absorption, a higher temperature increase can be expected, which may result in a lower rich loading. Introducing intercooling in the absorption step may thus be necessary to maintain a low temperature, and a high rich loading.

The physical solubility of CO_2, which determines how much CO_2 that dissolves in the solution, is often significantly higher in organic solvents than in water. Thus, the physical solubility of CO_2 in WLSs and NASs typically increases with increasing ratio of the organic solvent (Garcia et al., 2018). A higher physical solubility of CO_2 could in theory facilitate the reaction between CO_2 and the amine in solution due to more CO_2 being dissolved in the solution, and therefore being available for reaction.

The reaction pathways for CO_2 in an amine solution will vary depending on the functional groups and degree of steric hindrance of the amine and, of course, the solvent used. As described above, it has been proposed that MEA reacts via a zwitterionic species to form the MEA carbamate (Reactions 1-2). However, the water component also plays a role in the reactions; bicarbonate being the end-product (Reactions 3-8), increasing the loading slightly. Replacing the water component with an organic solvent will thus change the reaction pathways.

If the organic solvent itself does not participate in the reaction with CO_2, the overall reaction for non-aqueous MEA is reduced to that with the amine, according to Reaction 9. Compared to the case of aqueous MEA, the maximum theoretical loading would be slightly lower due to the lack of formation of bicarbonate. For

sterically hindered primary amines, such as AMP, this would mean a decrease in the maximum loading by half, compared to the aqueous case.

If hydroxyl groups are present in the organic solvent (alcohols) they can participate in the reaction with CO_2 forming the corresponding alkyl carbonate (Reaction 11), further increasing the maximum theoretical loading. The formation of solvent alkyl carbonates usually increases with increasing steric hindrance of the amine, due to the lower stability of the amine carbamate formed (Chowdhury et al., 2020).

$$CO_2 + RNH_2 + R'OH \leftrightarrow R'OCOO^- + RNH_3^+ \quad \{11\}$$

Changing to an organic solvent can thus reduce the rich loading of the system that can be achieved, but the possible lean loading may also decrease. Figure 3 shows the CO_2 solubility, at 40 and 120 °C, in non-aqueous solutions of MEA in solution with NMP (Wanderley et al., 2020a), MEG (monoethylene glycol) (Wanderley et al., 2020a) and EGME (2-methoxyethanol) (Guo et al., 2019). As can be seen, lower lean loadings can be achieved at lower partial pressures of CO_2 than in the aqueous MEA case (Figure 2). However, when organic solvents with boiling points above that required for desorption are used, the partial pressure of CO_2 in the regeneration column will be higher than when water vapor is present. Thus, in order to achieve lower lean loadings and increase the cyclic capacity, the CO_2 partial pressure must be kept low. This could be done by introducing an inert stripping gas during regeneration. However, this would alter the regeneration conditions, and several factors would have to be taken into account, such as the gas miscibility with the absorption solution, and how easy it is to separate it from the desorbed CO_2 (Wang et al., 2017).

The dielectric permittivity has been suggested to play a role in the shifting of the CO_2 loadings obtained towards lower equilibrium values when using organic solvents (Wanderley et al., 2019). Solvents with low dielectric permittivity are expected to lead to poor stabilization of the charged carbamate (Reaction 2) in the solution. Thus, carbamate formation will be less favored, shifting the equilibrium to the left, causing less CO_2 to be chemically absorbed in the solution (Wanderley et al., 2020a, 2019). The shift towards lower CO_2 loadings overall could have potential benefits, as amine-based absorption solutions typically become more corrosive as the CO_2 loading increases (Pearson and Cousins, 2016).

Another advantage of WLSs and NASs is their potential to lower the temperature needed for regeneration. Replacing water with amines that form sterically hindered carbamates can result in lower regeneration temperatures (80-90 °C) as further reaction to more stable reaction products can be limited by the choice of solvent (Barzagli et al., 2013b; Chowdhury et al., 2020; Svensson et al., 2014a). This means that low-grade heat can be used to regenerate the absorption solution.

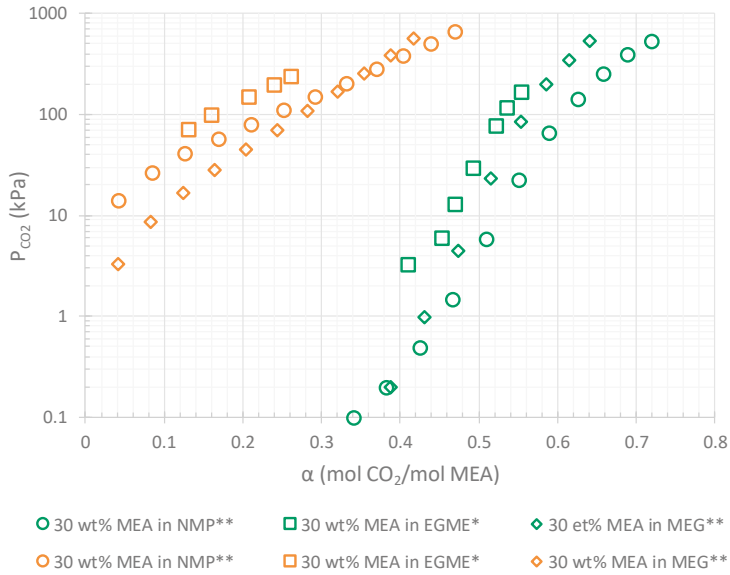

Figure 3. Literature data showing the solubility of CO_2 in non-aqueous MEA solutions at 40 °C (green) and 120 °C (orange). * (Wanderley et al., 2020a), ** (Guo et al., 2019)

2.3 Phase changing absorption systems

Phase-changing CO_2 absorption systems are reactive homogeneous liquid systems that separate into two phases as CO_2 is absorbed and reacts. A CO_2-rich phase that includes most of the absorbed CO_2 is formed from the reaction products, and a CO_2-lean phase that consists mainly of the solvent and physically absorbed CO_2. Depending on the nature of the CO_2 absorption system, phase-changing solvents can be divided into two categories, namely precipitating systems, where a new solid phase is formed from the reaction with CO_2 (turning the solution into a liquid/solid slurry), and bi-phasic liquid systems, where a new CO_2-rich phase, which is immiscible with the CO_2-lean phase, is formed. This separation into a lean and a rich phase is accompanied by the heat associated with the phase transition, and must be accounted for in the respective part of the capture process. The heat of regeneration for such systems is described by Eq. 2.3, where the heat of phase change (ΔH_{phase}) is included.

$$\Delta H_{reg} = \Delta H_{abs} + \Delta H_{sens} + \Delta H_{vap} + \Delta H_{phase} \qquad (2.3)$$

Separation into a CO_2-rich and a lean phase allows most of the absorbed CO_2 to be concentrated in one stream that is sent to the regeneration column, while the lean

phase is sent back to the absorption column without regeneration. Since regeneration is highly energy intensive, these types of systems have the potential to reduce the energy required for regeneration (Liang et al., 2015; Shen et al., 2017).

A simplified schematic of a process employing a phase-changing CO_2 absorption system is shown in Figure 4. The solution from the absorber passes through a separation unit where the rich phase is separated and sent to the stripper, and the lean phase is mixed with the regenerated solution and sent back to the absorption column.

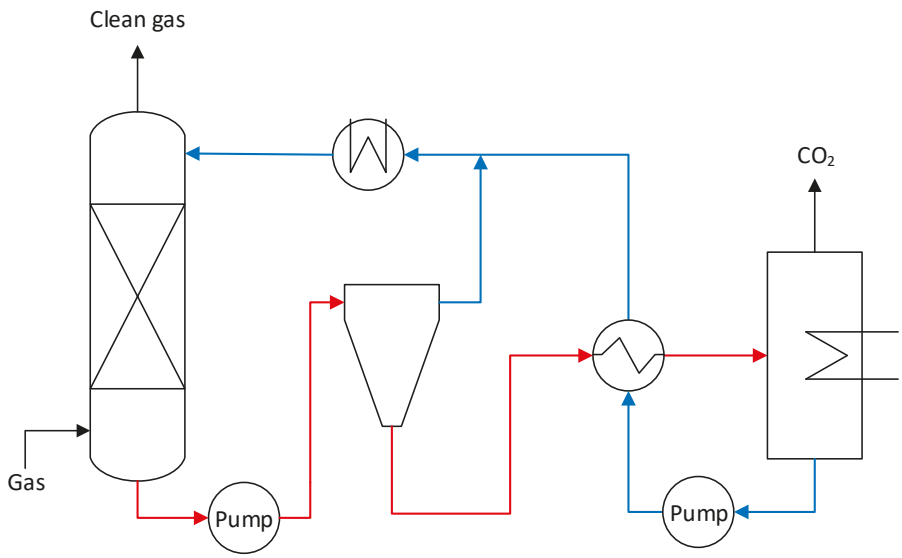

Figure 4. Schematic of a process employing a phase-changing absorption system, including an absorption column, rich/lean phase separation, regeneration and heat exchange between the CO_2-rich (red) and lean (blue) solution.

The unconventional design required for post-combustion carbon capture using phase-changing absorption systems is considered one of the major challenges associated with these types of systems (Budzianowski, 2017). Apart from the additional separation step, phase-changing systems can differ significantly from conventional aqueous systems, as alternative designs might be required for all the process units. Nevertheless, several pilot studies using phase-changing systems have been carried out in recent years. An example is the DMX™ process developed by IFP Energies nouvelles. This employs a bi-phasic liquid amine solution that separates into a CO_2-rich aqueous phase and a CO_2-lean organic phase that contains most of the amine. The phases are then separated after the heat exchanger so that only the rich phase is regenerated, thus reducing the heat duty compared to conventional process designs (Raynal et al., 2011). This system was successfully tested in a mini-pilot plant (Raynal et al., 2014), and is also being tested in an

industrial-scale pilot plant in a project ending in 2023 (CORDIS EU research results, 2020). Pilot studies have also been carried out demonstrating the use of precipitating potassium carbonate solutions where the solid precipitate was dissolved before the stripper (Aronu et al., 2018). A precipitating potassium carbonate solution has also been studied in a pilot plant using industrial flue gas, where a hydrocyclone was used to separate the lean and rich phases before the regeneration step (Smith et al., 2017).

2.4 Important properties of absorption solutions and methods used to evaluate them

The CO_2 solubility is one of the most important properties of a potential absorption solution, and is defined as the amount of CO_2 absorbed by the solution at a certain CO_2 partial pressure and temperature. It is usually determined by measuring the vapor–liquid equilibrium (VLE) of the system. The solubility of CO_2 usually decreases with increasing temperature. By collecting VLE data at temperatures and pressures that correspond to absorption and regeneration conditions, it is possible to estimate the potential rich and lean loadings that can be achieved at those conditions. From these data, it is then possible to estimate the cyclic capacity, which is the difference in rich and lean CO_2 loading at absorption and regeneration conditions, and gives an indication of the amount of solution that is needed to capture a certain amount of CO_2. The more solution that is needed to capture CO_2, the larger the process units must be, and the more energy is needed to heat the solution in the regeneration step. The solubility of CO_2 can be measured using various methods, provided that the distribution of a known amount of CO_2 between the gaseous and liquid phase can be determined.

The heat of absorption includes both the heat of dissolution and the heat of reaction. Physical and chemical absorption of CO_2 are both typically exothermic processes. The amount of heat released is important at the absorption stage, as this will lead to a temperature increase in the absorption column. If the heat of absorption is high, cooling of the solution during absorption will be necessary to avoid high temperatures that would reduce the rich loading and lower the overall cyclic capacity. The heat of absorption at regeneration temperatures is also important as it gives an indication of the amount of heat required to reverse the reaction, in order to desorb the CO_2. A low value of the heat of absorption could be beneficial, as this will give rise to a smaller temperature increase during absorption, and also less heat needed during CO_2 desorption in the regeneration step. However, the overall process design and other properties of the absorption solution, such as rate of reaction and loading capacity, which influence the solvent flow rate, also play important roles in the amount of heat required (Oexmann and Kather, 2010). The choice of method

used for the regeneration of an absorption solution can also be affected by the heat of absorption. For absorption solutions with a lower heat of absorption a pressure difference between the absorption and regeneration step (pressure swing) could be advantageous, whereas a temperature difference (temperature swing) could be advantageous for solutions with a higher heat of absorption (Oexmann and Kather, 2010).

The heat of absorption can be estimated from VLE data and the Gibbs-Helmholtz equation (Mathias and O'Connell, 2012). However, since the measurement error in the VLE data propagates in this type of calculation, resulting in high uncertainty in the estimated heat of absorption (Kim and Svendsen, 2007; Murrieta-Guevara et al., 1992), reaction calorimetry has become an established technique (Kierzkowska-Pawlak and Sobala, 2020; Mathonat et al., 1998; Wanderley et al., 2020b). This technique provides information on the VLE that can be used to estimate the solubility of CO_2 in an absorption solution. Since this technique also measures the heat flow needed to keep the temperature constant, it simultaneously allows for estimation of the heat of absorption.

The rate at which CO_2 is absorbed by a solution determines the necessary contact time between the incoming gas and the absorption solution. If the rate of absorption is low, a longer contact time will be needed, meaning a larger absorption column. The absorption rate is measured in terms of the CO_2 flux, from which the kinetic constants can be estimated. Common techniques to measure the absorption rate, involve counter-current setups, where a defined contact surface area can be obtained, and the concentration of CO_2 in the incoming gas is compared to that in the outgoing gas. Techniques such as the wetted wall column (WWC) (Lillia et al., 2018; Puxty et al., 2010; Yuan and Rochelle, 2018) or a string of discs (Aronu et al., 2011b) are commonly used. The rate of absorption is typically dependent on the concentration of both CO_2 and the amine. The reaction rate and kinetic constants can be estimated from the measured absorption rate. In order to facilitate these calculations, the experiments are often performed so that a pseudo-first-order (PFO) reaction can be assumed. This relies on the assumption that the reaction is fast, and that the concentration of the reactive amine is high enough to be considered constant at the gas–liquid interface and in the solution, throughout the experiment. The rate of absorption can also be estimated using a stirred cell reactor. In such setups, CO_2 is introduced into a batch reactor and the flux is estimated from the pressure decrease over time and the gas–liquid interfacial contact area (Kierzkowska-Pawlak, 2015). This method usually also uses the PFO assumption to facilitate the calculations. Semi-quantitative designs have also been used for fast screening and comparison of absorption rates where CO_2 is bubbled through the absorption liquid, and the gas–liquid interfacial area is unknown (Ma'mun et al., 2007).

The viscosity and volatility of the absorption solution are also important properties. The viscosity affects the diffusivity of dissolved species, which in turn affects the rate of absorption. If the viscosity is too high, the PFO assumption may not be valid,

as the diffusivity of the dissolved species will be too low. The viscosity also affects the heat transfer in the heat exchangers and the work needed to pump the solution (Rochelle, 2016; Wanderley et al., 2019). The volatility affects the solvent loss in the capture process. If the volatility is high, solvent traps are needed to reclaim the solvent that would otherwise be lost with the outgoing gas (Rochelle, 2016).

3 Methods

Many experimental methods commonly used to study liquid absorption systems cannot be used for precipitating absorption solutions. The formation of solid particles during the measurements complicates the evaluation of these types of systems. The work presented in this thesis focused mainly on the evaluation of non-aqueous absorption systems based on AMP. This chapter describes the main methods used and the experimental conditions, while the results obtained are presented in the next chapter.

3.1.1 Evaluation of the solubility of CO_2 and heat of absorption

All the data on the solubility and heat of absorption included in this thesis (**Papers I, II, III & V**) were obtained using a true heat flow reaction calorimeter (Chemical Process Analyser CPA 201, ChemiSens AB). The experimental setup is illustrated in Figure 5. A stirred batch reactor, made of glass and stainless steel, with a volume of 250 cm^3, was used in all the experiments. The amount of absorption solution was determined gravimetrically before being loaded into the reactor. Before each experiment, the reactor was evacuated at 25 °C for 10-12 s, after which the temperature was increased to the desired experimental temperature. The temperature was kept constant by a thermostat unit, using a water bath. The system was then allowed to equilibrate before CO_2 was introduced. The initial equilibrium pressure accounts for the remaining air and solvent vapor pressure of the unloaded solution and was assumed to remain constant throughout the duration of the experimental run. Equilibrium was assumed to have been reached when the signals for the total pressure and true heat flow deviated by less than 0.005 bar and 0.02 W, respectively, for approximately 30 min. CO_2 was then injected in a series of small doses using a mass flow controller (MFC), and the system was allowed to equilibrate between injections. The signals from the MFC, temperature, pressure and true heat flow sensors were logged throughout the experiment.

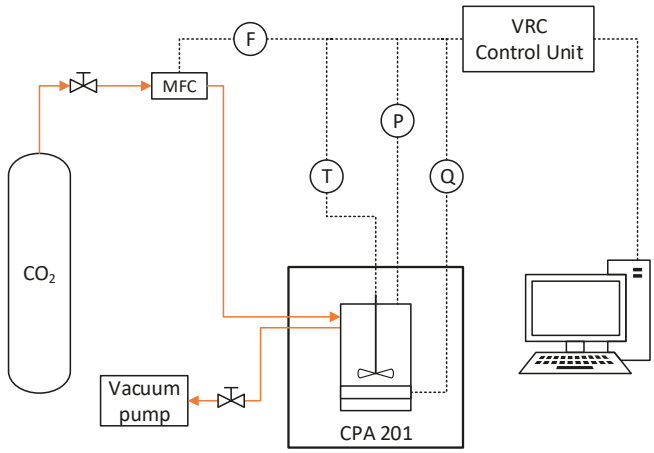

Figure 5. Schematic of the chemical process analyzer (CPA 201) experimental setup used for the calorimetric experiments. Gas (orange) was dosed using a mass flow controller (MFC) and signals from MFC flow (F), temperature (T), pressure (P) and true heat flow (Q), were continoulsy logged.

The data obtained from the calorimeter were evaluated as described previously (Svensson et al., 2014a, 2014c). The CO_2 partial pressure was estimated from the increase in total pressure resulting from each CO_2 injection. The amount of absorbed CO_2 ($(n_{CO2})_{abs}$) was estimated according to Eq. 3.1, as the difference between the amount of CO_2 added ($(n_{CO2})_{added}$) and the amount of CO_2 estimated to remain in the gaseous phase.

$$(n_{CO2})_{abs} = (n_{CO2})_{added} - \frac{P_{CO_2}V}{RT} \qquad (3.1)$$

where P_{CO2} is the partial pressure of CO_2, V is the volume of the gas above the liquid sample in the reactor, R is the molar gas constant and T is the temperature.

Henry's constant (H) was estimated for the different organic solvents according to Eq. 3.2, where x_{CO2} is the molar ratio of CO_2 in the solvent.

$$H = \frac{P_{CO2}}{x_{CO2}} \qquad (3.2)$$

For the reactive amine solutions, the CO_2 loading (α) expressed as mol CO_2/mol AMP was estimated according to Eq. 3.3.

$$\alpha = \frac{(n_{CO2})_{abs}}{(n_{AMP})_0} \qquad (3.3)$$

where $(n_{AMP})_0$ is the total molar amount of AMP in the solution.

The heat produced in the reactor (Q) was estimated by integrating the true heat flow signal. The heat of absorption ($-\Delta H_{abs}$) was then estimated as either the integral heat of absorption (Eq. 3.4), where the total amount of heat is divided by the total amount of absorbed CO_2, or the differential heat of absorption (Eq. 3.5), where the heat released after each injection is divided by the amount of CO_2 absorbed in that injection.

$$-\Delta H_{abs,int} = \frac{Q_{tot}}{(n_{CO2})_{abs}} \tag{3.4}$$

$$-\Delta H_{abs,diff} = \frac{dQ}{d(n_{CO2})_{abs}} \tag{3.5}$$

The method described above does not distinguish between physically and chemically absorbed CO_2 in the liquid phase. Nor does it distinguish between the CO_2 present in the liquid and in the solid precipitate, as it is not possible to determine how much precipitation forms during each CO_2 injection. Neither is it possible to distinguish between different reactions. Thus, the heat of absorption will be a collective value for all equilibria and reactions taking place as CO_2 is introduced into the system. For CO_2 absorption in precipitating AMP systems the heat of absorption thus includes the heat of dissolution, the heat of reaction and the heat of precipitation.

The uncertainties in the values obtained were calculated by statistical calculations to estimate the error propagation, taking into account the uncertainties in the individual measurements and steps in the sample preparation. The uncertainties varied for the different AMP solutions but were in general between 1-3% for the amount of CO_2 absorbed in the solutions, and between 1-4% for the heat of absorption values.

3.1.2 Absorption rate

A WWC was used to estimate the rate of absorption in a non-aqueous AMP solution (**Paper IV**). The overall experimental setup is shown in Figure 6, and a schematic of the WWC is shown in Figure 7. The WWC consists of a stainless-steel pipe, through which the absorption solution is pumped in from the bottom. The solution is evenly distributed over the outside of the pipe before it exits at the bottom of the column. The known dimensions of the pipe, and estimates of the area of the liquid film allow the liquid surface i.e., the contact area between the solution and gas, to be estimated. A gas mixture consisting of a CO_2, N_2 and He (inert standard) enter through three pipes at the bottom of the WWC, and exit at the top. The gases were dosed individually using MFCs, so that the CO_2 content in the gas mixture could be varied. Before the gas mixture entered the column, it was saturated by bubbling it

through either water or organic solvent, in the aqueous and non-aqueous experiments, respectively.

The liquid temperature was measured at both the inlet and outlet of the column. A Hiden analytical mass spectrometer (HAL IV RC RGA101) was used to analyze the gas composition. The amount of CO_2 absorbed was obtained from the difference in CO_2 pressure signal when gas either bypassed or passed through the WWC. The pressure signal was calibrated with the inert standard.

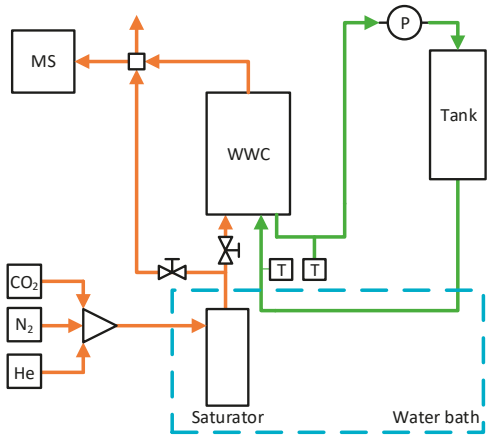

Figure 6. Schematic of the experimental setup used for the measurements with the wetted wall column (WWC) (Paper IV). The gas (orange) composition was analyzed using a mass spectrometer (MS) and the liquid solution (green) was circulated using a pump (P). Thermocouples (T) ware used to measure the temperature at the inlet and outlet of the WWC.

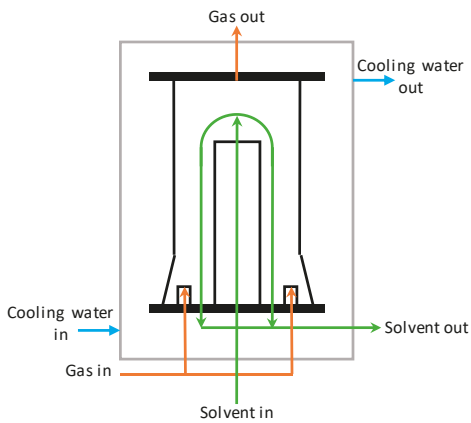

Figure 7. Schematic of the wetted wall column (WWC) used in the experiments described in Paper IV. Gas (orange) entered from pipes at the bottom of the column and exited from the top of the reactor. The liquid solution (green) entered through a stainless steel pipe and exited from the bottom of the column. The pipe is enclosed by glass walls held together by stainless steel plates.

The experiments were carried out using initially unloaded solutions to ensure that no precipitation would occur during the experiment, as this would have changed the estimated contact area. The CO_2 flux (N_{CO2}) was estimated by dividing the amount of CO_2 absorbed by the contact area. The two-film theory (Lewis and Whitman, 1924) was used, in which the physical absorption is described by CO_2 mass transfer in two steps, first through a gas film (from the gas bulk to the gas–liquid interface), then through a liquid film (from the interface to the liquid bulk), as illustrated in Figure 8. The CO_2 flux on the gaseous side (Eq. 3.6) is described by the gas-side mass transfer coefficient (k_g) and the CO_2 pressure difference between the gas bulk ($P_{CO2,bulk}$) and the interface ($P_{CO2,i}$). Similarly, the liquid-side CO_2 flux (Eq. 3.7) is described by the liquid-side mass transfer coefficient (k_l) and the CO_2 concentration difference between the interface ($C_{CO2,i}$) and the bulk liquid ($C_{CO2,bulk}$). The liquid side mass transfer coefficient includes the physical mass transfer coefficient (k_l^0) and the chemical reaction, which is accounted for through the enhancement factor (E). The difference in CO_2 concentration in the liquid film can be expressed in terms of CO_2 partial pressure, resulting in the right-hand side of Eq. 3.7, where the liquid-side mass transfer coefficient is now denoted k'_g. Combining Eqs. 3.6 and 3.7 results in the overall expression for the CO_2 absorption from the bulk gas to the bulk liquid, expressed in Eq. 3.8, where K_G is the overall mass transfer coefficient.

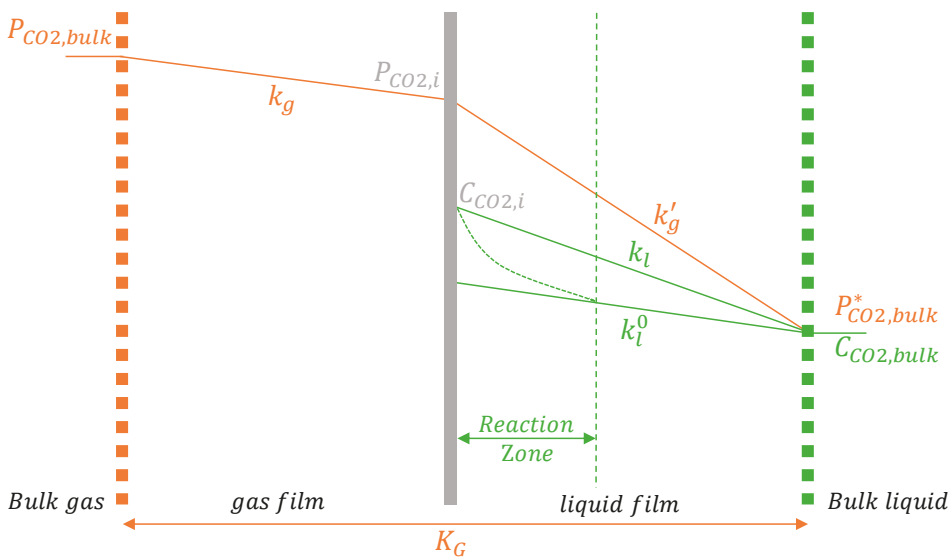

Figure 8. Illustration of the two-film theory, showing CO_2 mass transfer from the gas to the liquid bulk with fast chemical reactions. Adapted from (Dugas, 2009).

$$N_{CO2,g} = k_g\left(P_{CO2,bulk} - P_{CO2,i}\right) \tag{3.6}$$

$$N_{CO2,l} = k_l\left(C_{CO2,i} - C_{CO2,bulk}\right) = E \cdot k_l^0\left(C_{CO2,i} - C_{CO2,bulk}\right) = k_g'\left(P_{CO2,i} - P^*_{CO2,bulk}\right) \tag{3.7}$$

$$N_{CO2} = K_G\left(P_{CO2,bulk} - P^*_{CO2,bulk}\right) \tag{3.8}$$

The gas-side mass transfer in the column was first characterized using aqueous MEA, to determine k_g. The same gas conditions were then used for the experiments on the rate of absorption in the AMP solution. The overall mass transfer coefficient, K_G, was estimated from the CO_2 flux, from which the liquid-side mass transfer coefficient (k'_g) could then be estimated, according to Eq. 3.9.

$$\frac{1}{K_G} = \frac{1}{k_g} + \frac{H_{CO2}}{E \cdot k_l^0} = \frac{1}{k_g} + \frac{1}{k\prime_g} \tag{3.9}$$

If the experiments are performed with the assumption that the reaction is in the PFO regime, the second-order rate constant (k_2) can be estimated from the liquid-side mass transfer coefficient. This assumption can be made if the reaction is independent of the amine concentration, which is true if no depletion of amine occurs at the gas–liquid interface, and if the equilibrium reactions favor product formation, which is true if the equilibrium constant is high (Versteeg et al., 1996). A PFO reaction regime can be assumed if the conditions in Eq. 3.10 are met, i.e. if the Hatta number (Ha) is greater than 3 and much less than the infinite enhancement factor (E_∞) (Danckwerts, 1970).

$$3 < Ha \ll E_\infty \tag{3.10}$$

The Hatta number can be expressed by the second order rate constant (k_2), concentration of the amine ($C_{Amine,bulk}$), the diffusivity of CO_2 in the liquid ($D_{CO2,lq}$), and the physical mass transfer coefficient (k_l^0), according to Eq. 3.11.

$$Ha = \frac{\sqrt{k_2 \cdot C_{Amine,bulk} \cdot D_{CO2,lq}}}{k_l^0} \tag{3.11}$$

The infinite enhancement factor can be estimated according to Eq. 3.12, from the diffusivities of amine and CO_2 in the solution ($D_{Amine,lq}$ and $D_{CO2,lq}$), The bulk concentration of the amine ($C_{Amine,bulk}$) and the CO_2 concentration at the gas-liquid interface ($C_{CO2,i}$). ν_{Amine} is the ratio of amine to CO_2 from the reaction mechanism.

$$E_\infty = 1 + \frac{D_{Amine,lq} \cdot C_{Amine,bulk}}{\nu_{Amine} \cdot D_{CO2,lq} \cdot C_{CO2,i}} \tag{3.12}$$

3.1.3 Nuclear magnetic resonance

Carbon-13 nuclear magnetic resonance (^{13}C NMR) was used to investigate the chemical species in liquid non-aqueous AMP solutions (**Paper III**) and in AMP solutions with added water (**Paper V**). Before the experiment, AMP solutions were stirred under a $^{13}CO_2$ atmosphere for 30 min. Samples of the CO_2-containing solutions were then transferred to capped NMR tubes immediately before the measurements. Spectra were recorded for each sample, using either a Bruker or Varian 400 MHz spectrometer fitted with a 5 mm probe, at temperatures between 30 and 80 °C for the non-aqueous solutions, and between 30 and 88 °C for solutions containing water. For the non-aqueous samples, an average of 1024 scans, employing 20-degree pulses separated by 5 s delay, was used for each spectrum. For the samples with added water an average of 512 scans employing 20-degree pulses separated by 5 s delay, was used. In all measurements, DMSO-d_6 were used as a reference for the chemical shift.

As solid particles cannot be detected using this method, the amine concentration in the evaluated samples was kept low (below 10 wt% for AMP/DMSO and 2.5 wt% for AMP/NMP) to avoid precipitation during the measurements. As these low amine concentrations and the lack of precipitation would provide a low CO_2 capture capacity, any CO_2 absorption systems based on these components would be favored by a higher amine content. However, the results of the ^{13}C NMR measurements provide an indication of which chemical species are formed, as CO_2 reacts with AMP in either NMP or DMSO. Information can also be obtained on how the distribution of species in the solution changes with increasing temperature. The results can, however, not be directly translated to solutions with higher AMP concentrations, as reaction products formed by side reactions might not be detected.

4 Amine Absorption using AMP and Organic Solvents

The primary amine AMP was studied in different non-aqueous absorption formulations. AMP is a sterically hindered primary alkanolamine, and its structure is shown in Figure 9.

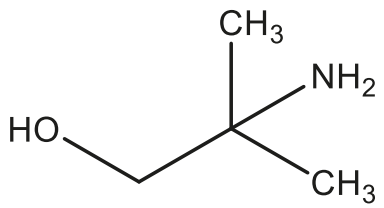

Figure 9. Chemical structure of 2-amino-2-methyl-1-propanol.

In a non-aqueous solution, AMP reacts with CO_2 according to Reactions 12-13. Physical absorption of CO_2 takes place according to Reaction 12 as the gaseous (g) CO_2 is dissolved in the liquid solution (sol). The AMP carbamate is then formed according to Reaction 13 as a result of the reaction between AMP and CO_2. If the solvent is not involved in the reaction, the maximum theoretical loading is limited to 0.5 mol CO_2/mol AMP.

$$CO_2(g) \rightleftarrows CO_2(sol) \quad \{12\}$$

$$CO_2(sol) + 2\,RNH_2(sol) \rightleftarrows RNH_3^+(sol) + RNHCOO^-(sol) \quad \{13\}$$

A higher CO_2 loading can be achieved if the solvent participates in the reaction. When alcohols are used as solvents, further reaction to the corresponding alkyl carbonate can occur, according to Reaction 14, with AMP as the counter-ion. The maximum theoretical loading in this case is 1 mol CO_2/mol AMP.

$$CO_2(sol) + RNH_2 + R'OH \rightleftarrows RNH_3^+(sol) + R'OCOO^-(sol) \quad \{14\}$$

If the solvent does not participate in the reaction, the steric hindrance of the AMP carbamate induces solid precipitation (s) of the carbamate salt, according to Reaction 15.

$$RNH_3^+(sol) + RNHCOO^-(sol) \rightleftarrows [RNH_3]^+[RNHCOO]^-(s) \qquad \{15\}$$

Several non-aqueous solvent formulations using AMP have been evaluated previously, including solutions with pure glycols (ethylene glycol (EG), diethylene glycol, triethylene glycol) (Zheng et al., 2013, 2012) and mixtures of linear alcohols (ethanol and propanol) with EG or diethylene glycol monomethyl ether (DEGMME) (Barbarossa et al., 2013; Barzagli et al., 2019, 2018, 2014, 2013b). However, many of these have focused on single-phase systems where there is no precipitation or it is prevented. Precipitation of the AMP carbamate has, however, been reported when pure propanol or DEGMME was used as the solvent (Barzagli et al., 2018, 2014, 2013b), while no precipitation was seen when using mixtures containing EG. Barzagli et al. also studied the regeneration of the solid AMP carbamate formed in solutions with ethylene glycol monoethyl ether, and found it could be decomposed into CO_2 and free amine at 80 °C (Barzagli et al., 2013a).

The research performed by our group has mainly focused on non-aqueous AMP systems that favor the formation and precipitation of the AMP carbamate. Previous work includes evaluation of the solubility of CO_2 (Svensson et al., 2014a) and heat of CO_2 absorption (Svensson et al., 2014c) in AMP/NMP and AMP/Triethylene glycol dimethyl ether (TEGDME) systems at 25 and 50 °C. The precipitate formed in these systems was evaluated and the main component was found to be the AMP carbamate (Svensson et al., 2014b). The crystallization kinetics of the AMP carbamate in AMP/NMP solutions has also been studied (Sanku and Svensson, 2017, 2020), and a model of the AMP/NMP system developed using ASPEN Plus® (Sanku and Svensson, 2019). The following sections describe the author's contributions to the work on AMP in solutions with organic solvents.

4.1 Solubility of CO_2 in AMP solutions

The solubility of CO_2 was studied in various systems containing AMP and organic solvents. The first system studied was AMP in mixtures with the organic solvent NMP (**Paper I**). NMP is used commercially for removal of acidic gases through physical absorption (PURISOL™) (Boll et al., 2011; Hochgesand, 1970). Two concentrations of AMP were studied: 15 and 25 wt% (denoted 15A-N and 25A-N, respectively), at temperatures from 40 to 88 °C. As NMP is reproductively toxic (European Chemicals Agency (ECHA), 2019), other solvents were investigated, with which precipitation could be obtained, in an attempt to find an alternative (**Paper II**). Seven solvents were investigated in mixtures with 25 wt% AMP namely,

DMSO, 1-pentanol (1P), 3-(dimethylamino)propionitrile (DMAPN), propylene carbonate, 4-heptanone, 1-methyl imidazole and cyclohexanol, at low temperatures (25-40 °C). DMSO showed promising solubility and precipitation properties, and a more detailed investigation of AMP with DMSO was therefore carried out (**Paper III**). Two concentrations of AMP in DMSO, 10 wt% (10A-D) and 25 wt% (25A-D), were investigated at temperatures between 25 and 88 °C.

The solubility of CO_2 in 15A-N and 25A-N at different temperatures is shown in Figure 10, including data at 25, 40, 50 and 88 °C from previously published studies by our group (Svensson et al., 2014a; Svensson and Karlsson, 2018). Precipitation was observed at 25-40 °C for 15A-N and at 25-50 °C for 25A-N. In general, the solubility of CO_2 was higher in 25A-N than in 15A-N at lower temperatures, mainly due to precipitation at lower loadings and lower CO_2 partial pressures. Precipitation drives the equilibrium reactions (12-15) to the right, which enables more CO_2 to be dissolved in the solution. Higher rich loadings can thus be obtained when precipitation occurs at low partial pressures of CO_2.

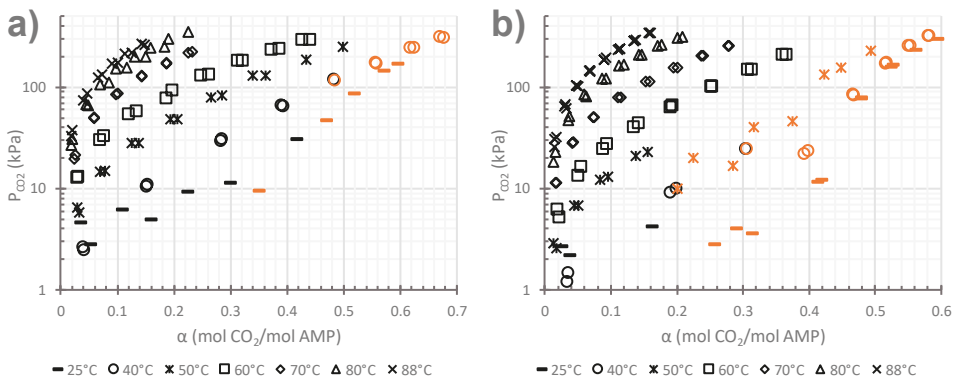

Figure 10. Solubility of CO_2 in **a)** 15 wt% AMP/NMP (15A-N) and **b)** 25 wt% AMP/NMP (25A-N), at 25-88 °C.* Data points at which precipitation was observed are shown in orange.

No precipitation was observed at temperatures of 60-88 °C. The difference in CO_2 solubility between 15A-N and 25A-N decreased with increasing temperature, and no significant difference was seen above 70 °C. At 88 °C, low loadings of approximately 0.05 mol CO_2/mol AMP were observed at partial pressures of 100 kPa, for both solutions. This suggests that low lean loadings can be achieved without the use of a stripping gas, at temperatures lower than the 120 °C used in conventional systems.

The rich loading obtained at 40 °C and 10 kPa was about 0.15 mol CO_2/mol AMP for 15A-N and 0.2 mol CO_2/mol AMP for 25A-N. With a lean loading of 0.05 (88 °C, 100 kPa), this corresponds to a cyclic capacity of 0.1 for 15A-N and 0.15 mol CO_2/mol AMP for 25A-N. This is low compared to aqueous MEA, where cyclic

capacities of around 0.3 mol CO_2/mol MEA can be achieved. Such low cyclic capacities would require the use of more than twice the amount of absorption solution to remove the same amount of CO_2 using AMP/NMP instead of aqueous MEA. This would likely increase the overall cost of carbon capture. In order to obtain loadings comparable to those obtained with aqueous MEA, higher partial pressures of CO_2 or a reduction in the absorption temperature to 25 °C or less would be required. Reducing the absorption temperature would, however, require additional cooling of the incoming gas and lean absorption solution. For 25A-N, loadings above 0.3 can be achieved at 40 °C for CO_2 partial pressures just above 20 kPa. This can be compared to the partial pressures of 60 kPa required at 40 °C for 15A-N. Thus, the cyclic capacity benefits from a higher amine concentration as this results in precipitation at lower loadings.

As NMP is toxic to reproduction, its use as a solvent in large scale processes is undesirable, as the low exposure limit (threshold value of 3.6 ppm during 8 h (Sigma-Aldrich, 2021)) would require extensive safety measures. Other solvents were therefore investigated in solutions with 25 wt% AMP. CO_2 solubility data for 25 wt% AMP in DMSO (25A-D), 1-pentanol (25A-1P) and DMAPN (25A-DMAPN) are shown in Figure 11. Precipitation was observed in all three systems, but the loading at which precipitation occurred varied. In 25A-DMAPN, precipitation was observed immediately upon the first injection of CO_2 at both 25 and 40 °C, whereas for 25A-1P and 25A-D precipitation only occurred at higher loadings, as can be seen in the figure. At 40 °C, the highest CO_2 solubility was observed in 25A-DMAPN and the lowest in 25A-1P. As discussed above, the solubility of CO_2 in precipitating systems is dependent on the loading at which precipitation occurs; precipitation at lower loadings resulting in higher solubility at lower CO_2 partial pressures. The difference in Henry's constant for CO_2 (a measure of the physical CO_2 solubility) differs for different organic solvents, and this will also probably affect the overall CO_2 solubility. The physical solubility of CO_2 decreases in the order DMAPN > DMSO > 1P, and the same trend can be seen in the solubility data in Figure 11 at 40 °C.

The immediate precipitation observed in 25A-DMAPN indicates low stability of the CO_2 reaction products formed in the solvent, and suggests that the solution is less prone to be supersaturated. However, it also means that precipitation will take place at the low loadings of a lean solution. For precipitating solutions, precipitation at somewhat higher loadings could be beneficial, as this could allow precipitation in a designated part of the absorption column.

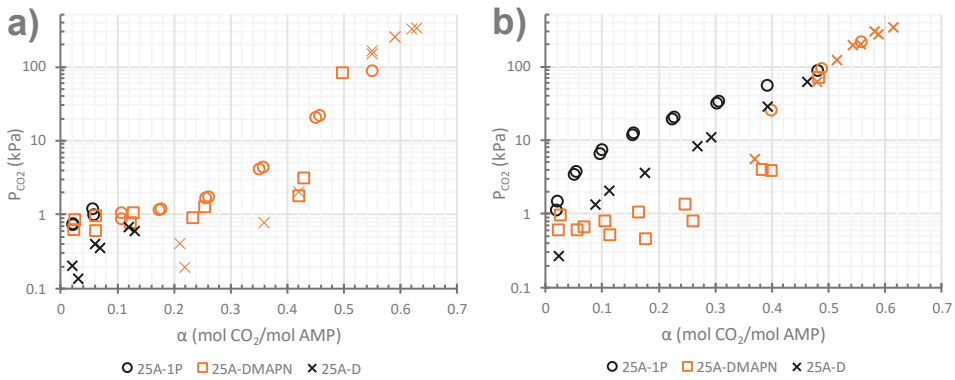

Figure 11. Solubility data for 25 wt% AMP in 1P (25A-1P), DMSO (25A-D) and DMAPN (25A-DMAPN) at **a)** 25 °C and **b)** 40 °C.* Data points at which precipitation was observed are shown in orange.

Among the amine solutions studied, the system of AMP in DMSO was chosen for further evaluation, as it had a high boiling point (189 °C) and showed solubility trends similar to those in the AMP in NMP system (**Paper II**). Figure 12 shows the solubility of CO_2 in 10A-D and 25A-D at various temperatures. No precipitation was observed within the pressure and temperature ranges studied when using 10A-D. Precipitation was observed with 25A-D at 25-50 °C, similar to the 25A-N system. At 25 °C, loadings of about 0.4 mol CO_2/mol AMP were obtained at CO_2 partial pressures below 3 kPa. The main difference between the 10A-D and 25 A-D systems is seen at lower temperatures (25-50 °C), where the precipitation in 25A-D resulted in higher loading at lower partial pressures. No precipitation was observed at 60-88 °C in either of the solutions. Similar to the case of the AMP/NMP system, the difference between the solubility of CO_2 in 10A-D and 25A-D decreased with increasing temperature, and no significant difference was seen above 80 °C. In general, the solubility of CO_2 was slightly higher in 25A-D than in 25A-N, at all temperatures. At 88 °C and 100 kPa, loadings of about 0.08 mol CO_2/mol AMP were obtained for both 10A-D and 25A-D.

To obtain a cyclic capacity similar to that obtained with aqueous MEA (above 0.3 mol CO_2/mol amine), rich loadings of about 0.4 mol CO_2/mol AMP are thus required. This can be achieved at 40 °C when the CO_2 partial pressure is above 40 kPa for 10A-D and between 10 and 30 kPa for 25A-D. Thus, the solubility data suggest that 25A-D might be more suitable for carbon capture at lower CO_2 partial pressures than 25A-N.

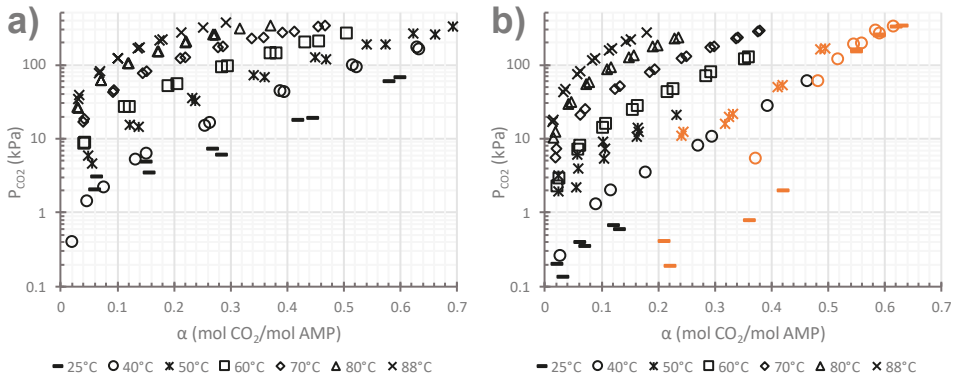

Figure 12. Solubility data for **a)** 15 wt% AMP/DMSO (15A-D) and **b)** 25 wt% AMP/DMSO (25A-D), at 25-88 °C.* Data points at which precipitation was observed are shown in orange.

From the solubility data collected for AMP in solutions with NMP and DMSO, it can be seen that low lean loadings below 0.1 mol CO_2/mol AMP can be achieved for these systems at CO_2 a partial pressure of 100 kPa and a temperature of 88 °C. This means that concentrated CO_2 streams could be obtained at lower temperatures than those needed for the stripping of conventional aqueous systems (120 °C). From the data in Figure 12, it can be seen that precipitation is necessary in order to obtain cyclic capacities that can compete with those of conventional aqueous systems. At a typical absorption temperature of 40 °C, this is achieved at CO_2 partial pressures around 20 kPa. In post-combustion applications when treating flue gases from the power sector, the CO_2 content is typically below 15 kPa. Thus, the systems described in this thesis are more suitable for biogas upgrading and CCS in industries where the gases have a higher CO_2 content.

Since no precipitation was observed at 60 °C, and the AMP systems must precipitate to attain sufficient cyclic capacities, the temperature increase in the absorption column must be kept as low as possible. As the reactions taking place during absorption (Reactions 12-15) are exothermic, the solution will most likely require intercooling during absorption in order to avoid desorption in the absorption column. Cooling of the incoming gas and lean solution to 25 °C to reduce the maximum temperature is another alternative. However, this will add to the cooling demand, which might result in an increase in the electricity required for the process.

From the perspective of CCS, the possibility of generating pressurized CO_2 during regeneration could be of interest, as this could significantly reduce the compression work needed after the capture process to attain pressures suitable for CO_2 transport and storage (up to 150 bar). A higher CO_2 pressure during regeneration will, however, also result in higher lean loadings of the absorption solution during the regeneration step. This can be seen in Figure 13, where the solubility of CO_2 in 25A-D solutions initially loaded to 0.5 mol CO_2/mol AMP at 25 °C before being heated

to 88 °C, is shown together with the solubility data for 25A-D (from Figure 12) at 40 and 88 °C. For rich solutions with a loading of 0.48 mol CO_2/mol AMP at 40 °C (60 kPa), a CO_2 pressure above 600 kPa was achieved at 88 °C and loadings of 0.36 mol CO_2/mol AMP. This corresponds to a cyclic capacity of 0.12, which is significantly lower than the cyclic capacity of 0.4 obtained when regeneration was performed at 88 °C and CO_2 pressures of 100 kPa. This reduction in capacity would drastically increase the amount of solvent needed to remove a specific amount of CO_2, and would probably not be commercially feasible. However, if lean and rich phases are separated before the regeneration step, lower lean loadings might be possible, as the solvent after regeneration would be mixed with the CO_2-lean phase before being returned to the absorption column. However, further studies are needed to determine whether this is feasible for the 25A-D system.

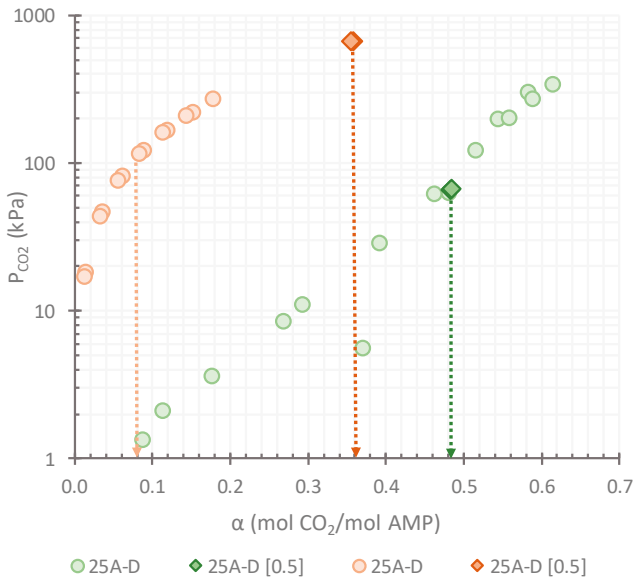

Figure 13. Solubility of CO_2 in 25A-D solutions at 40 °C (green) and 88 °C (orange). Comparison between initially unloaded solutions (circles) and solutions initially loaded to 0.5 mol CO_2/mol AMP at 25 °C (diamonds).

In systems where precipitation does not occur immediately upon the first injection of CO_2, the conditions at which precipitation takes place can be determined from the pressure and true heat flow data. This is shown in Figure 14a, where the true heat flow and pressure signals from a typical data series during precipitation, are plotted.

Exothermic precipitation leads to higher values of the estimated heat of absorption due to the increased heat flow. In the vast majority of the obtained equilibrium data, precipitation was followed by a decrease in pressure, as can be seen in the pressure

curve of Figure 14a. This is because precipitation drives the equilibrium equations (Reactions 12-15) to the right, which allows more CO_2 to be dissolved in the solution. However, in some cases, when precipitation occurs at CO_2 loadings around 0.5 mol CO_2/mol AMP, corresponding to the maximum theoretical loading, the measured pressure increases, as can be seen in Figure 14b. Changes in the liquid properties could explain this deviation in behavior. When precipitation occurs close to the theoretical maximum loading, most or all of the AMP in solution will likely be included in the solid precipitate, whereas if precipitation occurs at lower loadings, significant amounts of AMP, and corresponding ionic species, will remain in the solution. This will probably cause significant changes in the properties of the liquid solution, resulting in changes in parameters such as pH, viscosity, Henry's constant and the dielectric constant, all of which affect the solubility of CO_2.

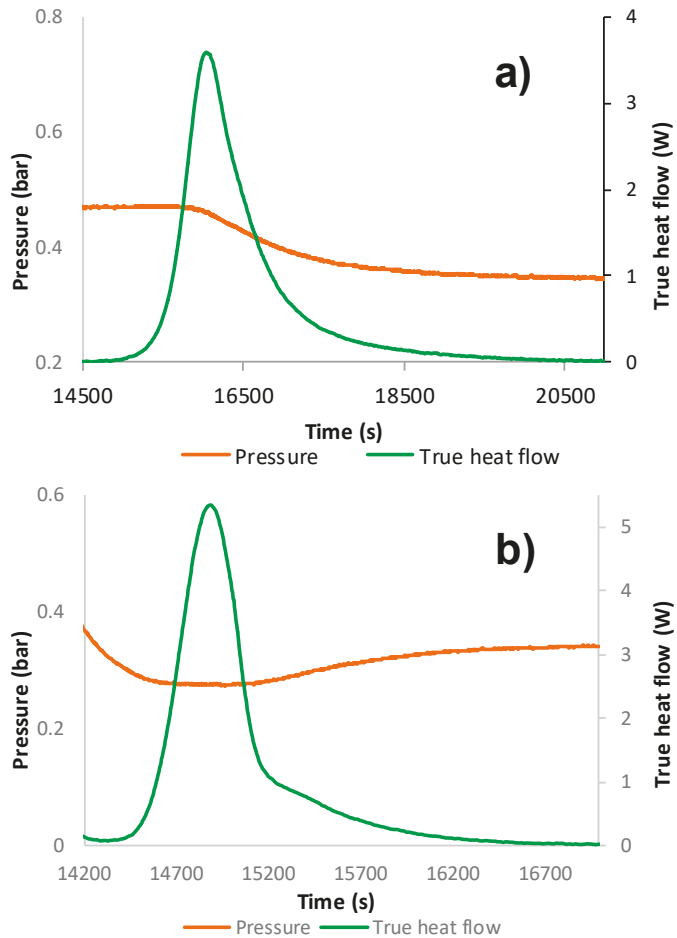

Figure 14. Pressure and heat flow during precipitation in non-aqueous AMP solutions. a) Decreasing pressure during precipitation, b) Increasing pressure during precipitation.

4.2 Heat of absorption

The heat of absorption was obtained by integrating the measured true heat flow signal, collected simultaneously with the solubility data presented in the previous section. Estimating the heat of absorption from the measured true heat flow signal allows both the integral and differential heat of absorption to be determined, according to Eqs. 3.4 and 3.5. To obtain the integral heat of absorption, the accumulated heat is divided by the accumulated amount of absorbed CO_2 at each loading. The differential value of the heat of absorption is calculated from the heat added and the CO_2 absorbed at each data point. In both cases, a value is obtained for each data point. However, in the integral heat of absorption, any spikes in the heat of absorption are averaged out between the data points, whereas the differential value will show more realistic values for each point. As the precipitation processes in the AMP solutions studied in this work are exothermic, the heat of absorption will be higher than in the non-precipitating case. Three mechanisms thus contribute to the overall heat of absorption for precipitating systems: the heat of dissolution, the heat of reaction and the heat of precipitation.

Figure 15 shows the differential heat of absorption at different loadings for 15A-N and 25A-N. Values obtained in previously published work (at 25 and 50 °C), are also included (Svensson et al., 2014c). It can clearly be seen that the heat of absorption increases considerably as precipitation occurs, for both 15A-N and 25A-N, where the values above 150 kJ/mol CO_2 correspond to the point where most of the precipitation took place. These high values indicate that the solution is supersaturated when precipitation takes place. As more precipitation takes place simultaneously in a supersaturated solution than in the non-supersaturated equilibrium case, more heat is released at this single point than if it was evenly distributed over the entire loading range.

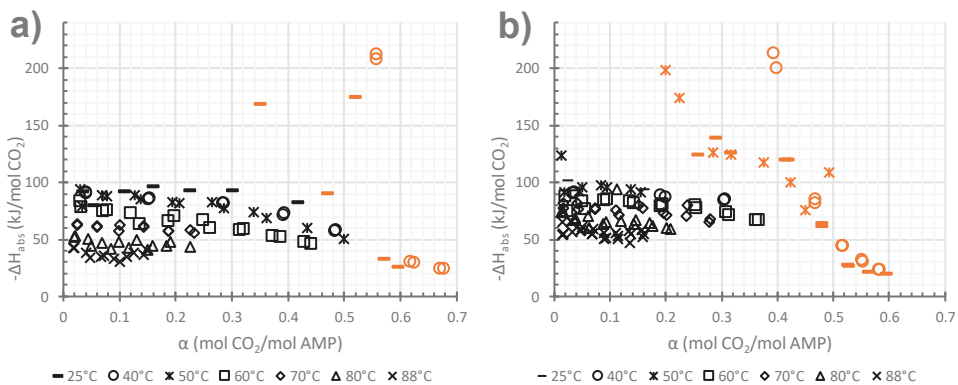

Figure 15. Differential heat of CO_2 absorption as a function of loading in **a)** 15 wt% AMP/NMP (15A-N) and **b)** 25 wt% AMP/NMP (25A-N), at 25-88 °C. Data points at which precipitation was observed are shown in orange.

Similar supersaturated trends, resulting in a significantly higher heat of absorption, can be observed for 25A-D in Figure 16b. For 10A-D (Figure 16a), where no precipitation was observed during the experiment, the heat of absorption decreased with increasing loading, similarly to other non-precipitating systems. For all the systems studied, the heat of absorption above a loading of 0.5 mol CO_2/mol AMP approaches that of physical absorption (where only the heat of dissolution contributes) as the theoretical maximum reaction capacity has been reached above this loading. The heat of physical absorption is about 5-6 times lower than the heat of chemical absorption, with values between 14 and 19 kJ/mol CO_2 for both NMP and DMSO.

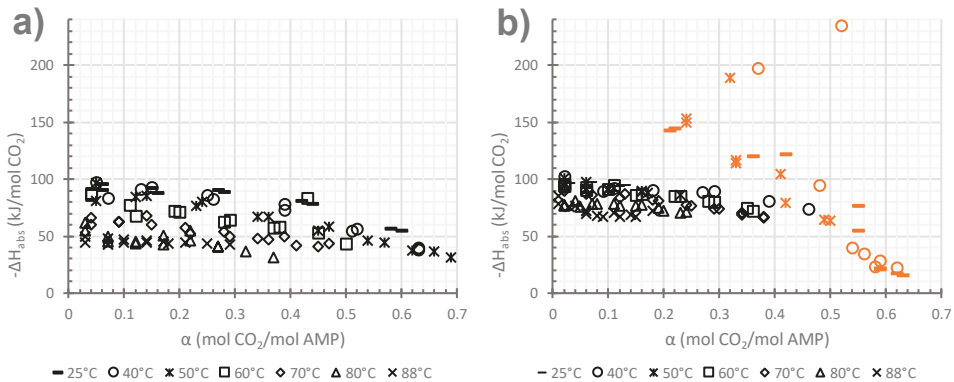

Figure 16. Differential heat of CO_2 absorption as a function of loading in **a)** 10 wt% AMP/DMSO (15A-D) and **b)** 25 wt% AMP/DMSO (25A-D), at 25-88 °C. Data points at which precipitation was observed are shown in orange.

Above 50 °C, the heat of absorption starts to decrease with increasing temperature. The reason for this is believed to be that the dissolved CO_2 species in solution are shifting from a higher proportion being chemically reacted, to a higher proportion being physically dissolved (This is further discussed in Section 4.4). The decrease is more apparent at lower amine concentrations (15A-N vs. 25 A-N and 10A-D vs. 25A-D), probably due to the higher proportion of organic solvent.

Since the precipitating solutions discussed above were supersaturated before the initial precipitation point, the contribution of the precipitation heat to the overall heat of absorption cannot be estimated from these data alone. However, a rough estimate of the heat of precipitation can be made by comparing these systems to other AMP solutions in which precipitation occurs immediately upon the first injection of CO_2, thus not showing supersaturation behavior. Figure 17 shows the heat of absorption for several 25 wt% AMP solutions at temperatures between 25 and 50 °C. The data for 25A-N and 25A-D represent the supersaturated solutions, and include values with and without precipitation. Data are also included for 25A-DMAPN, 25wt% AMP in 4-heptanone (25A-4H) and 25wt% AMP in

TEGDME (25A-T) (Svensson et al., 2014c), representing the non-supersaturated solutions in which precipitation occurs immediately. It can clearly be seen that the average value of the heat of absorption varies between the solutions with and without precipitation. Apart from the very high values obtained at the initial precipitation point for the supersaturated systems, the heat of absorption for data points with precipitation (shown in orange) has an average value of 122 kJ/mol CO_2 at temperatures between 25 to 50 °C. The average value for data points without precipitation (shown in black) is about 90 kJ/mol CO_2. If one assumes that the organic solvents do not participate in the reaction, and that all the AMP carbamate in the non-supersaturated solutions precipitates as it is formed, the difference between these values would then be the heat of precipitation, giving an approximate value of 30 kJ/mol CO_2.

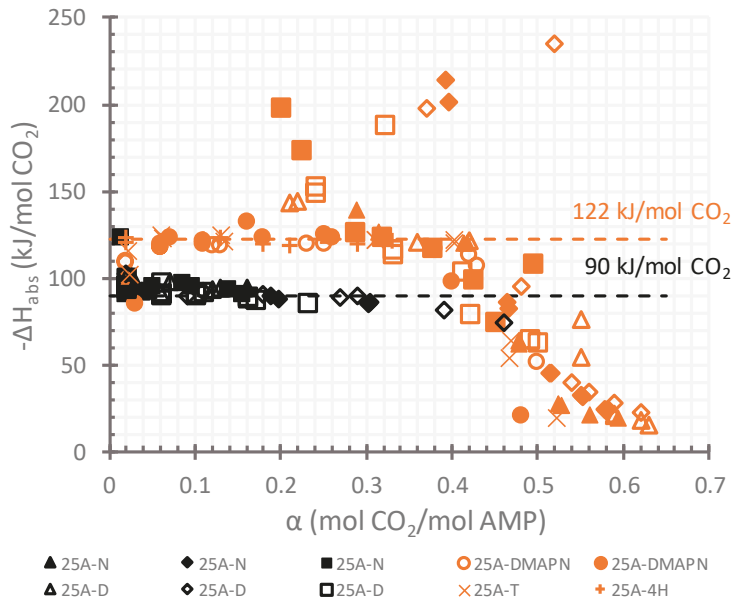

Figure 17. Differential heat of absorption for CO_2 in solutions with 25 wt% AMP in different organic solvents at 25-50 °C. Data points at which precipitation was observed are shown in orange.

The heat of absorption affects the temperature profile in the absorption column, as the heat released will increase the solvent temperature. The additional heat released due to precipitation will cause a greater temperature increase in precipitating systems, than in non-precipitating systems. This could be more pronounced in non-aqueous systems, as organic solvents typically have a lower heat capacity (below 2.0 kJ/(kg·K) for both NMP (Dávila and Trusler, 2009) and DMSO (Comelli et al., 2006)) than water (approx. 4.2 kJ/(kg·K)). Additionally, some of the heat released during absorption in aqueous systems will contribute to the evaporation of water,

thus reducing the temperature increase slightly. In the case of non-volatile solvents with high boiling-point, where evaporation occurs to a lesser extent, the temperature increase may be even more pronounced. Thus, non-aqueous precipitating absorption systems will most likely require cooling of the solution during the absorption step to keep the temperatures within the range suitable for absorption.

Another challenge is associated with solutions that are prone to become super-saturated. In contrast to non-supersaturated solutions, where the additional precipitation heat will be distributed over the entire loading range, supersaturated solutions will experience a significant heat release once precipitation is initiated. This may cause local hot spots in the column, where the temperature is increased to the point where the equilibrium is shifted towards desorption. However, if the absorption column can be designed such that precipitation is achieved in a designated part of the column, the additional heat release could be manageable by more extensive temperature control on this part of the column.

During the regeneration step, the heat of absorption contributes to the heat needed to reverse the reactions and desorb CO_2. The heat of precipitation will add to this heat requirement, as the solid particles formed must be re-dissolved in the solution. However, the benefits associated with using these types of solutions are not intended to lower the heat of absorption. The main advantages are associated with the low regeneration temperature, potentially enabling the use of excess heat for the regeneration step, and lowering the contribution of the sensible heat and heat of vaporization during regeneration.

4.3 Rate of absorption

The rate of absorption affects the contact time and area needed to remove a certain amount of CO_2 in the absorption column. A higher absorption rate is advantageous since it allows for a smaller contact area, and thus a smaller absorption column. The rate of absorption of CO_2 in AMP and NMP solutions was studied and compared with that in aqueous MEA, at 27 °C (**Paper IV**). Two concentrations of AMP in NMP were investigated, 1.5 m and 5 m (11.8 and 30.8 wt% (30A-N)), and compared to aqueous MEA with concentrations of 1.5 m and 7 m (8.4 and 30.0 wt% (30M-W)).

The average values of the liquid-side mass transfer coefficient (k'_g) at room temperature, estimated from the CO_2 flux at different CO_2 partial pressures, are given in Table 1 for 30A-N and 30M-W. Under the PFO assumption, the second-order rate constants (k_2) can be estimated from the mass transfer coefficient, and are also presented in Table 1. The values of k_2 presented here includes any side reactions taking place, such as formation of bicarbonate from CO_2 reacting with hydroxyl ions in the 30M-W solution.

Table 1. Mass transfer (k'_g) and second-order rate constants (k_2) at approximately 27 °C.

Solution	k'_g [mol/(m²·s·Pa]	k_2 [m³/(s·mol)]
30A-N	$2.72 \cdot 10^{-6}$	5.3
30M-W	$2.03 \cdot 10^{-6}$	7.3

The values obtained indicate that the mass transfer of CO_2 into the liquid solution is higher for 30A-N than for 30M-W. This is probably the result of the difference in physical solubility between the two systems. The physical solubility of CO_2 is about 4 times higher in AMP/NMP than in aqueous MEA, based on estimated values of Henry's constant (792 and 3292 Pa·m³/mol at 25 °C for 25A-N and 30M-W, respectively) (Karlsson and Svensson, 2018). Higher mass transfer rates than for aqueous solutions have been reported for several absorption mixtures where water has been replaced with organic solvents with a higher physical solubility of CO_2 (Garcia et al., 2018; Wanderley et al., 2019; Yuan and Rochelle, 2018).

The estimates of the second-order rate constants show the opposite behavior, being higher for 30M-W than for 30A-N. This indicates a slower reaction with AMP than with MEA in their respective solutions. It should be noted that the molar amine concentration differs between the solutions, 4.9 vs. 3.5 M for 30M-W and 30A-N, respectively. AMP in aqueous solutions has also been reported to have a slower reaction rate than aqueous MEA; k_2 being one order of magnitude higher than that of AMP (6.83 vs. 0.681 m³/(s·mol) at 28 °C (Saha et al., 1995)). However, the value of k_2 for AMP in 30A-N found in this work (Table 1) is almost 10 times higher than that obtained for aqueous AMP at similar temperatures, and on the same order of magnitude as that found for MEA. Several assumptions were made to obtain the rate constant for 30A-N, e.g., regarding the diffusivity of both CO_2 and AMP in the solution, and the value in Table 1 should be regarded as a rough first estimate. It might, however, be that the PFO assumption is not actually valid under the conditions studied, and further investigations are needed to determine this. Since k_2 is obtained from the mass transfer coefficients, a higher k_2 for 30A-N than for aqueous AMP is however expected since the physical solubility of CO_2 is higher than in the aqueous solution.

The results given in Table 1 were obtained using initially unloaded solutions. However, this does not reflect the conditions in the absorption column, as the solution entering the column will have the lean loading resulting from the regeneration step, which will gradually increase as absorption proceeds. As the AMP carbamate precipitates, within the loading range expected in the absorption column, the WWC technique can no longer be used to evaluate the absorption rate. The formation of solid particles will obstruct the liquid film in the column such that the contact area between the gas and liquid cannot be correctly estimated. From the solubility data discussed in Section 4.1, it can, however, be seen that it is possible

to achieve very low lean loadings of 0.05 mol CO_2/mol AMP in the regeneration of AMP/NMP mixtures. This value is similar to the theoretical loadings estimated from the experimental conditions in the study described in **Paper IV**. It is thus likely that the rate of absorption in the top of the absorption column, where the lean absorption solution enters the absorption step, is comparable to that estimated in experiments with initially unloaded solutions. However, the absorption rate that applies to the rich solution cannot be estimated for precipitating absorption systems using techniques that require the laminar flow of a liquid film for the estimation of the contact area, as discussed above. Other methods must be used to study this, and a stirred cell reactor could be one possible alternative (Kierzkowska-Pawlak, 2015).

The PFO assumption is also often applied to the stirred cell reactor approach to determine kinetic parameters. However, the PFO assumption might not be applicable when using WLS and NAS. The absorption of CO_2 in the liquid leads to an increase in the viscosity of the solution. The viscosity affects the diffusivity of the species in the solution, and will thus affect the absorption rate. This was investigated in the WWC by measuring the CO_2 flux (N_{CO2}) at constant partial pressure (P_{CO2}) and estimating the theoretical loading of the solution. The flux showed a decrease of 12% at loadings of 0.08 mol CO_2/mol AMP, compared to the unloaded solution, which could be the result of increasing viscosity. The higher viscosities for WLS and NAS have resulted in concerns regarding the validity of the PFO assumption in such systems (Wanderley et al., 2019; Yuan and Rochelle, 2018). If the diffusivity of the dissolved species is limited, this could lead to the depletion of free amine at the gas–liquid interface. In such a case, the assumption that the mass transfer rate is independent of amine concentration is no longer applicable.

4.4 Reaction products

In order to verify that the reaction products formed between AMP and CO_2 were those predicted by the proposed reaction mechanism, and to investigate any possible side reactions, ^{13}C NMR was used to determine which species were present in the liquid solution. Non-aqueous AMP solutions with amine concentrations at which precipitation could be avoided were used (**Paper III**).

The regions of the ^{13}C NMR spectra for the products and for physically dissolved CO_2, for CO_2 absorbed in 10A-D at temperatures between 30 and 80 °C, are shown in Figure 18. Three main species were identified as CO_2 reaction products at 30 °C. The peaks were assigned to: (1) the AMP carbamate, (2) bicarbonate formed from water, and (3) tentatively the AMP carbonate formed from reaction with the hydroxyl group of AMP. The peak appearing at lower shifts (4) is assigned to physically dissolved CO_2. The intensity of the peaks corresponding to the chemically reacted CO_2 species (1-3) starts to decrease as the temperature increases. The

broadening of the peaks implies dynamic interactions between the species in solution. At higher temperatures, the equilibrium reactions (12-13) will be shifted towards the left, which can be seen in Figure 18, as the peaks corresponding to reaction products (1-3) start to overlap the peak for physically dissolved CO_2 (4).

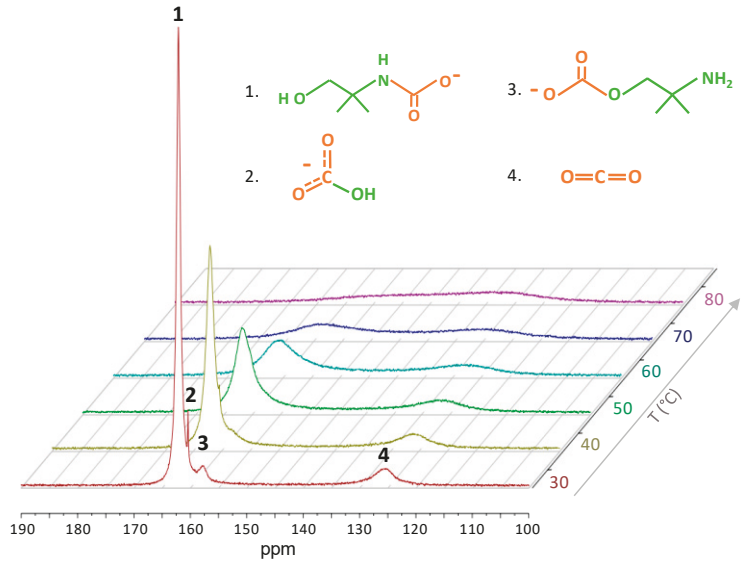

Figure 18. ^{13}C NMR spectra at 30-80 °C, showing CO_2-related species in solutions of 10A-D. The peaks are assigned as follows: (1) AMP carbamate, (2) bicarbonate, (3) AMP carbonate (tentative) and (4) physically dissolved CO_2.

The ratio between chemically reacted and physically dissolved CO_2 changes with temperature. A higher proportion of physically dissolved CO_2 than chemically reacted CO_2 can be seen at 80 °C than at 30 °C. This explains the decreasing trend in the heat of absorption as the temperature is increased, as discussed in Section 4.2. The heat of absorption is a combination of the heat of dissolution and the heat of reaction, according to Eq. 2.1. The heat released by CO_2 reactions is significantly higher than the heat released by CO_2 dissolution. If less CO_2 undergoes reactions at higher temperatures, the combined heat of absorption can be expected to decrease.

4.5 Influence of water

The solubility of CO_2 in mixtures of AMP and DMSO with added water was evaluated (**Paper V**). The hygroscopic properties of DMSO will probably result in the accumulation of water in any AMP/DMSO system, as the gas entering the process usually contains some water (5-10% in biogas (Angelidaki et al., 2018)). As

water enables the formation of bicarbonate, according to Reaction 10, a higher water content would mean a higher maximum theoretical CO_2 loading. However, further reaction to bicarbonate would result in less AMP carbamate in the solution. This could result in no precipitation of the carbamate, which, for the NASs studied in this work, could mean a reduced cyclic capacity.

Solutions of 100 g 25A-D to which either 5 or 10 g water was added (24A-D5W and 23A-D9W) were studied using reaction calorimetry in order to investigate the effect of water on CO_2 absorption. Figure 19 shows the CO_2 solubility in 25A-D, 24A-D5W and 23A-D9W at 40 and 88 °C. A shift towards higher CO_2 loadings at lower CO_2 partial pressure can be seen for the solutions with added water, at both 40 and 88 °C. This was expected, as the solubility of CO_2 increases with the formation of bicarbonate. Precipitation was observed in one of two runs using 24A-D5W and in both runs using 23A-D9W. This implies that, although further reaction to bicarbonate occurs, precipitation is still possible in these absorption systems. This suggests that some water can be tolerated in a NAS of AMP/DMSO, while still functioning as a precipitating absorption system.

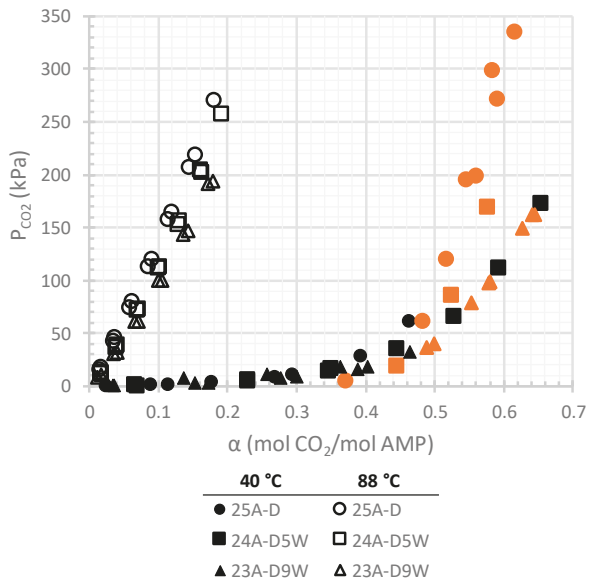

Figure 19. Solubility of CO_2 in 25A-D, 24A-D5W and 23A-D9W at 40 and 88 °C. Data points at which precipitation was observed are shown in orange.

The formation of bicarbonate was also confirmed using ^{13}C NMR, showing that a higher water content resulted in more bicarbonate being formed and less AMP carbamate. At some point, this will lead to a critical water concentration where an insufficient amount of AMP carbamate is present in solution for precipitation to

occur. The absorption solution would then have to be dried to ensure precipitation. Further studies are needed on water accumulation, as some water might be vaporized and removed in the regeneration step. Drying of the incoming gas may be necessary depending on how quickly water is accumulated.

Figure 20 shows the product region and the region for physically dissolved CO_2 of the ^{13}C NMR spectra for CO_2 absorbed in 10A-D4W, at temperatures between 30 and 88 °C, and again at 30 °C after heating. As in the case of the 10A-D solution (Figure 18), the main species in solution at 30 °C before heating are the AMP carbamate, bicarbonate, the tentatively assigned AMP carbonate, and physically dissolved CO_2. A new peak is seen at 80 °C, at a shift of 158 ppm, which was not seen in the spectrum for CO_2 in 10A-D at the same temperature. This peak is tentatively assigned to one of the potential degradation products of AMP, 4,4-dimethyl-1,3-oxazolidin-2-one (DMOZD), formed by ring closure of the AMP carbamate. The formation of DMOZD is irreversible, and the peak is still seen in the spectrum after the sample has been cooled to 30 °C. Apart from the new species detected, the main difference between 10A-D4W and 10A-D is the higher content of bicarbonate present in the solution, which requires higher temperatures to regenerate. This can be seen in the spectra as the bicarbonate peak is still present at temperatures up to 80 °C. However, at 88 °C the equilibrium reactions have shifted such that most of the CO_2 in solution is physically dissolved.

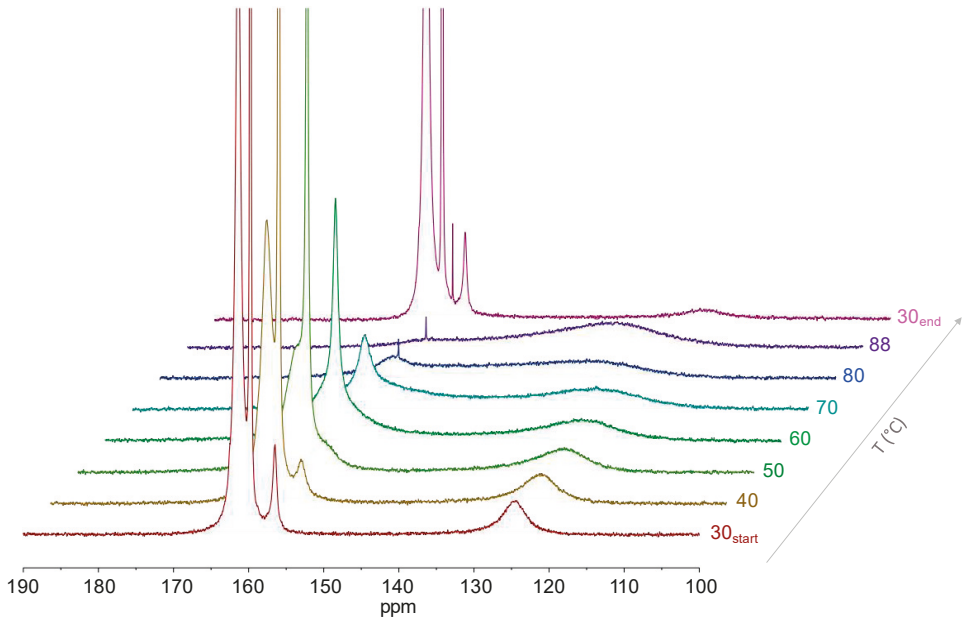

Figure 20. ^{13}C NMR spectra at 30-88 °C, showing CO_2-related species in solutions of 10A-D4W.

The combined results of the CO_2 solubility (Figure 19) and the ^{13}C NMR analysis (Figure 20) suggest that some water accumulation could be tolerable in an AMP/DMSO system, as a regeneration temperature of 88 °C can still be used to reverse the equilibrium reactions, while maintaining the cyclic capacity of the system. However, the appearance of a new species suggests that the accumulation of water might result in faster degradation of AMP into DMOZD. Further studies of both the non-aqueous and aqueous systems are needed in order to investigate this.

As discussed previously (Section 2.2), the presence of some water in an absorption solution might also be beneficial in the absorption step. The heat of absorption will result in a greater temperature increase than in aqueous systems, due to the lower specific heat capacity of DMSO and the additional heat of precipitation. In order to avoid reaching desorption temperatures, intercooling during the absorption step will probably be needed. The extent of cooling needed might be reduced by some water content in the solution due to the high heat of vaporization of water. Another potential benefit of a small amount of water in the system is depression of the freezing point. In colder climates a high freezing point of absorption solutions could cause complications during start up and shut down of the capture process and in storage of the solution. The freezing point of pure DMSO is around 18 °C, and decreases with increasing water content; 9% water resulting in a freezing point of -3 °C (Havemeyer, 1966). Further investigations are needed to determine the freezing point of tertiary systems of AMP/DMSO/H_2O. Overall, it is clear that water accumulating in AMP/DMSO solutions will alter the absorption behavior and properties of the solution. To what extent water will accumulate in such solutions needs to be evaluated under more realistic absorption and regeneration conditions.

5 Conclusions

The research described in this thesis focused on the evaluation of non-aqueous precipitating absorption solutions, using AMP. Several AMP solutions with different organic solvents were studied at potential absorption temperatures of 25-40 °C. Two systems, AMP/NMP and AMP/DMSO, were studied at both absorption and regeneration temperatures (< 90 °C). The solubility of CO_2 in these systems was found to be lower than in aqueous 30 wt% MEA, at all the temperatures studied. Conventional systems and non-aqueous precipitating AMP systems differ considerably, and thus their areas of application will differ. Therefore, the absorption and regeneration conditions most suitable for AMP/NMP and for AMP/DMSO were investigated (**RQ1**).

Both AMP/NMP and AMP/DMSO can be regenerated at low temperatures without the need for a stripping agent, with lean loadings below 0.1 mol CO_2/mol AMP at a temperature of 88 °C and atmospheric CO_2 pressure. Lower regeneration temperatures can thus be used in these non-aqueous systems than in conventional systems, allowing the use of low-grade heat in the regeneration step. This could reduce the cost of fuel for the regeneration of the absorption solution in industries where such heat is available. If no stripping agent is required, the need for condensation after regeneration could also be reduced, as less solvent will vaporize than when stripping aqueous amine solutions.

The absorption of CO_2 in both AMP/NMP and AMP/DMSO was found to be promoted by a higher amine concentration, as shown by the higher CO_2 loadings observed at lower CO_2 partial pressures in solutions with 25 wt% AMP than in the 15 and 10 wt% solutions. This is due to a higher amount of formed AMP carbamate, which results in precipitation at both lower CO_2 loadings and higher temperatures for 25A-N and 25A-D than for 15A-N, and the lack of precipitation in 10A-D. Precipitation of the AMP carbamate generates additional heat which, in combination with the low specific heat capacities of the organic solvents used, will most likely result in a greater increase in the temperature of the absorption solution during absorption than in conventional aqueous non-precipitating solutions. In order to use 25A-N and 25A-D solutions as bi-phasic absorption systems, the temperature during the absorption stage must be ≤50 °C as no precipitation was observed at 60 °C in any of the solutions studied. Intercooling of the absorption solution during the absorption step would otherwise be necessary, adding to the overall cooling demand of the capture process.

Although the overall solubility of CO_2 is lower in 25A-N and 25A-D than in aqueous 30 wt% MEA, it is possible to achieve similar CO_2 capture capacities (cyclic capacity) under the appropriate absorption conditions. The partial pressure of CO_2 affects the rich CO_2 loading that can be achieved during absorption; a higher partial pressure of CO_2 promoting precipitation at higher temperatures. At absorption temperatures around 40 °C, cyclic capacities similar to those in 30 wt% MEA can be achieved above a CO_2 partial pressure of 20 kPa for both 25A-N and 25A-D. If absorption is performed at 25 °C similar capacities can be achieved at 10 kPa with 25A-N and as low as 1 kPa with 25A-D. This suggests that if absorption is performed at around 40 °C, both 25A-N and 25A-D are more suitable for carbon capture in applications such as biogas upgrading and CCS in industry, where the CO_2 content is higher than in post-combustion scenarios in power production. However, if absorption could be performed at 25 °C, both systems could be utilized in scenarios with lower CO_2 concentrations.

Water accumulation arising from the hygroscopic properties of organic solvents may pose challenges, as water in incoming humid gases would accumulate over time, unless the incoming gas, or solvent, is dried. Water leads to the formation of bicarbonate, and thus a change in the CO_2 reaction products formed in the solution. If the water content in the absorption solution becomes too high, insufficient AMP carbamate would be available in solution for precipitation to occur, potentially reducing the capture capacity of the absorption system. Precipitation was still formed with CO_2 absorption in 25A-D solutions where water had been added at a molar ratio of water:AMP of 2:1. The solubility data also showed that a temperature of 88 °C could be sufficient for regeneration of the water-containing system. Thus, some water accumulation seems to be acceptable without reducing the capacity of AMP/DMSO, but further studies are required to investigate this.

The potential benefits of using non-aqueous AMP systems for carbon capture (**RQ2**) are associated with the regeneration of the absorption solution. Reducing the regeneration temperature used in conventional systems such as aqueous MEA, of 120 °C or above, to 90 °C, would allow the use of excess heat, which is often available in industry. This would reduce the energy required to produce heat for the regeneration step. Also, replacing the water component by NMP or DMSO, both of which have boiling points above the regeneration temperature, and lower specific heat capacities than water, would lower the sensible heat and heat of vaporization needed for regeneration. Furthermore, the precipitation of the AMP carbamate allows for a separation step to be introduced before regeneration, in which some of the organic solvent can be removed, thus creating a CO_2-rich slurry. This could lead to an additional reduction in the amount of heat needed for regeneration, as less solvent would have to be heated. It should also be noted that NMP is toxic to reproduction, and it would therefore be more suitable to use DMSO in future studies on non-aqueous precipitating AMP solutions.

The combination of lower regeneration temperatures, reduced contributions from sensible heat and heat of vaporization, together with an overall reduction in solvent flow in the regeneration step, provides the opportunity to reduce the heat needed in the CO_2 capture process. However, the use of non-aqueous precipitating solutions will result in a need to change the process configuration, requiring other process units than in traditional aqueous systems. The cooling demand during the absorption step is likely to increase as it would be necessary to keep the temperature of the solution within the precipitating range. Because of the higher viscosity of a liquid/solid slurry compared to a liquid solution, more work will be needed to pump the slurry. A higher viscosity will also affect the heat transfer efficiency, potentially reducing the degree of heat integration possible within the process, which could in turn result in an increase in the external heating needed. Additional energy would also be required by separation units needed to separate the lean and rich phases before the regeneration step. Thus, further investigations and modelling of the entire process are needed to evaluate the effects of using non-aqueous AMP solutions on the cost of a future carbon capture plant.

6 Future work

The non-aqueous precipitating AMP solutions, AMP/NMP and AMP/DMSO, studied within the framework of this thesis, offer an alternative technology to conventional carbon capture using aqueous amine solutions. The results indicated benefits such as lower desorption temperatures, allowing the use of excess heat in the regeneration step. In addition, precipitating solutions offer the possibility of separating the lean absorption solution before the regeneration step, reducing the amount of solvent that has to be heated. However, much work remains to determine whether they are suitable for industrial use, and whether they can compete with conventional aqueous solutions.

More accurate determination of the rate of absorption is needed to be able to estimate the contact times needed for different capture scenarios. This includes finding a method that can be applied when a solid precipitate is formed, as the methods currently used for kinetic evaluations of absorption systems are designed for non-precipitating solutions. The absorption rate must be evaluated at temperatures and CO_2 partial pressures relevant for the intended use, to obtain a realistic estimate of the absorption rate. The solutions must also be studied in continuous operation to evaluate their properties and the behavior of the precipitate. Large-scale testing of the system in a pilot plant with more relevant gas mixtures must also be performed. This is important to investigate the extent of water accumulation, and the effects this could have on the absorption solution over time. Furthermore, if the absorption solution is to be separated into a lean and rich phase before the regeneration step, studies must be carried out on the regeneration of the precipitate in mixtures with varying solvent contents.

The environmental impact of these systems must also be assessed by studying properties such as the volatility and degradation of the amine and organic solvents. The degradation of AMP in non-aqueous solutions must be investigated to determine the extent of amine loss and whether any harmful degradation products are formed during operation. The volatility of both the amine and organic solvent must also be further studied on pilot-plant scale, at absorption and regeneration temperatures, to determine the loss of absorption solution during the capture process.

References

Aaron, D., Tsouris, C., 2005. Separation of CO2 from flue gas: A review. Sep. Sci. Technol. 40, 321–348. https://doi.org/10.1081/SS-200042244

Al Seadi, T., Rutz, D., Janssen, R., Drosg, B., 2013. Ch.2 - Biomass resources for biogas production, in: The Biogas Handbook. Woodhead Publishing Limited, pp. 19–50. https://doi.org/10.1533/9780857097415.1.19

Angelidaki, I., Treu, L., Tsapekos, P., Luo, G., Campanaro, S., Wenzel, H., Kougias, P.G., 2018. Biogas upgrading and utilization : Current status and perspectives. Biotechnol. Adv. 36, 452–466. https://doi.org/10.1016/j.biotechadv.2018.01.011

Angelidaki, I., Xie, L., Luo, G., Zhang, Y., Oechsner, H., Lemmer, A., Munoz, R., Kougias, P.G., 2019. Ch.33 - Biogas Upgrading: Current and Emerging Technologies, in: Biofuels: Alternative Feedstocks and Conversion Process for the Production of Liquid and Gaseous Biofuels. Elsevier Inc., pp. 817–843.

Arachchige, U.S.P.R., Melaaen, M.C., 2013. Alternative solvents for post combustion carbon capture. Int. J. Energy Environ. 4, 441–448.

Aronu, U.E., Gondal, S., Hessen, E.T., Haug-Warberg, T., Hartono, A., Hoff, K.A., Svendsen, H.F., 2011a. Solubility of CO2 in 15 , 30 , 45 and 60 mass% MEA from 40 to 120 C and model representation using the extended UNIQUAC framework. Chem. Eng. Sci. 66, 6393–6406. https://doi.org/10.1016/j.ces.2011.08.042

Aronu, U.E., Hartono, A., Svendsen, H.F., 2011b. Kinetics of carbon dioxide absorption into aqueous amine amino acid salt: 3-(methylamino)propylamine/sarcosine solution. Chem. Eng. Sci. 66, 6109–6119. https://doi.org/10.1016/j.ces.2011.08.036

Aronu, U.E., Kim, I., Haugen, G., 2014. Evaluation of energetic benefit for solid-liquid phase change CO2 Absorbents. Energy Procedia 63, 532–541. https://doi.org/10.1016/j.egypro.2014.11.058

Aronu, U.E., Pellegrin, R., Hjarbo, K., Chikukwa, A., Kim, I., Tobiesen, A., Hargrove, B., Mejdell, T., 2018. Integrated phase change solvent-contactor process for CO2 scrubbing from industrial exhaust gases : Pilot plant demonstration, in: 14th Greenhouse Gas Control Technologies Conference Melbourne 21-26 October 2018 (GHGT-14). SSRN. pp. 1–3.

Aspelund, A., Jordal, K., 2007. Gas conditioning-The interface between CO2 capture and transport. Int. J. Greenh. Gas Control 1, 343–354. https://doi.org/10.1016/S1750-5836(07)00040-0

Barbarossa, V., Barzagli, F., Mani, F., Lai, S., Stoppioni, P., Vanga, G., 2013. Efficient CO2 capture by non-aqueous 2-amino-2-methyl-1-propanol (AMP) and low temperature solvent regeneration. RSC Adv. 3, 12349–12355. https://doi.org/10.1039/c3ra40933c

Barzagli, F., Giorgi, C., Mani, F., Peruzzini, M., 2019. Comparative Study of CO2 Capture by Aqueous and Nonaqueous 2-Amino-2-methyl-1-propanol Based Absorbents Carried Out by 13C NMR and Enthalpy Analysis. Ind. Eng. Chem. Res. 58, 4364–4373. https://doi.org/10.1021/acs.iecr.9b00552

Barzagli, F., Giorgi, C., Mani, F., Peruzzini, M., 2018. Reversible carbon dioxide capture by aqueous and non-aqueous amine-based absorbents : A comparative analysis carried out by 13C NMR spectroscopy. Appl. Energy 220, 208–219. https://doi.org/10.1016/j.apenergy.2018.03.076

Barzagli, F., Lai, S., Mani, F., 2013a. CO2 capture by liquid solvents and their regeneration by thermal decomposition of the solid carbonated derivatives. Chem. Eng. Technol. 36, 1847–1852. https://doi.org/10.1002/ceat.201300225

Barzagli, F., Lai, S., Mani, F., Stoppioni, P., 2014. Novel Non-aqueous Amine Solvents for Biogas Upgrading. Energy and Fuels 28, 5252–5258. https://doi.org/10.1021/ef501170d

Barzagli, F., Mani, F., Peruzzini, M., 2013b. Efficient CO2 absorption and low temperature desorption with non-aqueous solvents based on 2-amino-2-methyl-1-propanol (AMP). Int. J. Greenh. Gas Control 16, 217–223. https://doi.org/10.1016/j.ijggc.2013.03.026

Boll, W., Hochgesand, G., Higman, C., Supp, E., Kalteier, P., Müller, W.-D., Kriebel, M., Schlichting, H., Tanz, H., 2011. Gas Production, 3. Gas Treating. Ullmann's Encycl. Ind. Chem. https://doi.org/10.1002/14356007.o12_o02

Budzianowski, W.M., 2017. Ch.2 - Precipitating Solvents, in: Energy Efficient Solvents for CO2 Capture by Gas-Liquid Absorption: Compounds, Blends and Advanced Solvent Systems. Springer International Publishing, pp. 72–77.

Butler, J.H., 2013. CO2 at NOAA's Mauna Loa Observatory reaches new milestone: Tops 400 ppm [WWW Document]. Global Monitoring Division - ESRL-GMD. URL https://www.esrl.noaa.gov/gmd/news/7074.html (accessed 2.17.21).

Caplow, M., 1968. Kinetics of Carbamate Formation and Breakdown. J. Am. Chem. Soc. 90, 6795–6803. https://doi.org/10.1021/ja01026a041

Chowdhury, F.A., Goto, K., Yamada, H., Matsuzaki, Y., 2020. A screening study of alcohol solvents for alkanolamine-based CO2 capture. Int. J. Greenh. Gas Control 99, 103081. https://doi.org/10.1016/j.ijggc.2020.103081

Cigni, A., Dejean, E., Degrange-Meunier, S., de Wit, J., Florisson, O., Franek, J., Hec, D., Jönsson, O., Klaas, U., Lander, D., Scartazzini, S., Seifert, M., Seveno, E., Straka, F., Vinck, H., 2006. Injection of Gases from Non-Conventional Sources into Gas Networks (WG-Biogas-06-18).

Comelli, F., Francesconi, R., Bigi, A., Rubini, K., 2006. Excess molar enthalpies, molar heat capacities, densities, viscosities, and refractive indices of dimethyl sulfoxide + 1-propanol at (288.15, 298.15, and 308.15) K and at normal pressure. J. Chem. Eng. Data 51, 1711–1716. https://doi.org/10.1021/je0601513

CORDIS EU research results, 2020. DMX Demonstration in Dunkirk [WWW Document]. URL https://cordis.europa.eu/project/id/838031 (accessed 3.4.21).

Danckwerts, P.V., 1970. Gas-Liquid Reactions. McGraw-Hill Book Company, New York, USA.

Danckwerts, P. V., 1979. The reaction of CO2 with ethanolamines. Chem. Eng. Sci. 34, 443–446. https://doi.org/10.1016/0009-2509(79)85087-3

Dávila, M.J., Trusler, J.P.M., 2009. Thermodynamic properties of mixtures of N-methyl-2-pyrrolidinone and methanol at temperatures between 298.15 K and 343.15 K and pressures up to 60 MPa. J. Chem. Thermodyn. 41, 35–45. https://doi.org/10.1016/j.jct.2008.08.003

Deng, L., Liu, Y., Wang, W., 2020. Biogas Technology. Springer, Singapore.

Dlugokencky, E., Tans, P., 2021. Trends in Atmospheric Carbon Dioxide [WWW Document]. NOAA/GML. URL https://www.esrl.noaa.gov/gmd/ccgg/trends/global.html (accessed 5.6.21).

Dugas, R.E., 2009. Carbon Dioxide Absorption , Desorption , and Diffusion in Aqueous Piperazine and Monoethanolamine. The University of Texas at Austin.

European Chemicals Agency (ECHA), 2019. 1-methyl-2-pyrrolidone: Substance information [WWW Document]. URL https://echa.europa.eu/substance-information/-/substanceinfo/100.011.662 (accessed 10.04.21).

Feron, P.H.M., 2016. Ch.1 - Introduction, in: Absorption-Based Post-Combustion Capture of Carbon Dioxide. Elsevier Ltd, pp. 3–12. https://doi.org/10.1016/B978-0-08-100514-9.00001-9

Feron, P.H.M., Cousins, A., Jiang, K., Zhai, R., Garcia, M., 2020. An update of the benchmark post-combustion CO2-capture technology. Fuel 273, 117776. https://doi.org/10.1016/j.fuel.2020.117776

Garcia, M., Knuutila, H.K., Aronu, U.E., Gu, S., 2018. In fluence of substitution of water by organic solvents in amine solutions on absorption of CO2. Int. J. Greenh. Gas Control 78, 286–305. https://doi.org/10.1016/j.ijggc.2018.07.029

Guo, H., Shi, X., Shen, S., 2019. Solubility of N2O and CO2 in non-aqueous systems of monoethanolamine and glycol ethers: Measurements and model representation. J. Chem. Thermodyn. 137, 76–85. https://doi.org/10.1016/j.jct.2019.05.017

Haugen, H.A., Aagaard, P., Kjärstad, J., Bergmo, P.E.S., Nielsen, L.H., Eldrup, N.H., Skagestad, R., Mathisen, A., Thorsen, T.A., Johnsson, F., Bjørnsen, D., 2013. Infrastructure for CCS in the Skagerrak/Kattegat region, Southern Scandinavia: A feasibility study. Energy Procedia 37, 2562–2569. https://doi.org/10.1016/j.egypro.2013.06.139

Havemeyer, R.N., 1966. Freezing Point Curve of Dimethyl Sulfoxide - Water Solutions. J. Pharm. Sci. 55, 851–853.

Heldebrant, D.J., Koech, P.K., Glezakou, V., Rousseau, R., Malhotra, D., Cantu, D.C., 2017. Water-Lean Solvents for Post-Combustion CO2 Capture: Fundamentals, Uncertainties, Opportunities, and Outlook. Chem. Rev. 117, 9594–9624. https://doi.org/10.1021/acs.chemrev.6b00768

Hochgesand, G., 1970. Rectisol and Purisol. Ind. Eng. Chem. 62, 37–43. https://doi.org/10.1021/ie50727a007

IEA, 2021. Global Energy Review 2021. Paris. https://doi.org/https://www.iea.org/reports/global-energy-review-2021

Jou, F.-Y., Mather, A.E., Otto, F.D., 1995. The Solubility of CO2 in a 30 Mass Percent

Monoethanolamine Solution. Can. J. Chem. Eng. 73, 140–147. https://doi.org/https://doi.org/10.1002/cjce.5450730116

Karlsson, H., Svensson, H., 2018. Physical properties of the 2-amino-2-methyl-1-propanol and N-methyl-2-pyrrolidone system, in: 14th Greenhouse Gas Control Technologies Conference Melbourne 21-26 October 2018 (GHGT-14). SSRN, pp. 1–7.

Kierzkowska-Pawlak, H., 2015. Kinetics of CO2 absorption in aqueous N,N-diethylethanolamine (DEEA) and its blend with N-(2-aminoethyl)ethanolamine using a stirred cell reactor. Int. J. Greenh. Gas Control 37, 76–84. https://doi.org/10.1016/j.ijggc.2015.03.002

Kierzkowska-Pawlak, H., Sobala, K., 2020. Heat of absorption of CO2 in aqueous solutions of DEEA and DEEA + MAPA blends—A new approach to measurement methodology. Int. J. Greenh. Gas Control 100, 103102. https://doi.org/10.1016/j.ijggc.2020.103102

Kim, I., Svendsen, H.F., 2007. Heat of absorption of carbon dioxide (CO2) in monoethanolamine (MEA) and 2-(aminoethyl)ethanolamine (AEEA) solutions. Ind. Eng. Chem. Res. 46, 5803–5809. https://doi.org/10.1021/ie0616489

Klackenberg, L., 2020. Produktion och användning av biogas och rötrester år 2019 (ER 2020:25).

Knudsen, J.N., Andersen, J., Jensen, J.N., Biede, O., 2011. Evaluation of process upgrades and novel solvents for the post combustion CO2 capture process in pilot-scale. Energy Procedia 4, 1558–1565. https://doi.org/10.1016/j.egypro.2011.02.025

Knuutila, H.K., Nannestad, Å., 2017. Effect of the concentration of MAPA on the heat of absorption of CO2 and on the cyclic capacity in DEEA-MAPA blends. Int. J. Greenh. Gas Control 61, 94–103. https://doi.org/10.1016/j.ijggc.2017.03.026

Lackner, K.S., Park, A.H.A., Miller, B.G., 2010. Ch 6 - Eliminating CO2 Emissions from Coal-Fired Power Plants, in: Generating Electricity in a Carbon-Constrained World. 1st ed. Elsevier Inc. https://doi.org/10.1016/B978-1-85617-655-2.00006-7

Le Moullec, Y., Neveux, T., 2016. 13 - Process modifications for CO2 capture, in: Feron, P.H.M. (Ed.), Absorption-Based Post-Combustion Capture of Carbon Dioxide. Woodhead Publishing, pp. 305–340. https://doi.org/https://doi.org/10.1016/B978-0-08-100514-9.00013-5

Lewis, W.K., Whitman, W.G., 1924. Principles of Gas Absorption. Ind. Eng. Chem. 16, 1215–1220. https://doi.org/10.1021/ie50180a002

Liang, Z., Rongwong, W., Liu, H., Fu, K., Gao, H., Cao, F., Zhang, R., Sema, T., Henni, A., Sumon, K., Nath, D., Gelowitz, D., Srisang, W., Saiwan, C., Benamor, A., Al-Marri, M., Shi, H., Supap, T., Chan, C., Zhou, Q., Abu-Zahra, M., Wilson, M., Olson, W., Idem, R., Tontiwachwuthikul, P., 2015. Recent progress and new developments in post-combustion carbon-capture technology with amine based solvents. Int. J. Greenh. Gas Control 40, 26–54. https://doi.org/10.1016/j.ijggc.2015.06.017

Lillia, S., Bonalumi, D., Fosbøl, P.L., Thomsen, K., Valenti, G., 2018. Experimental study of the aqueous CO2-NH3 rate of reaction for temperatures from 15 °C to 35 °C, NH3 concentrations from 5% to 15% and CO2 loadings from 0.2 to 0.6. Int. J. Greenh. Gas Control 70, 117–127. https://doi.org/10.1016/j.ijggc.2018.01.009

Lin, Y., Chen, E., Rochelle, G.T., 2016. Pilot plant test of the advanced flash stripper for CO2 capture. Faraday Discuss. 192, 37–58. https://doi.org/10.1039/c6fd00029k

Lin, Y.J., Rochelle, G.T., 2016. Approaching a reversible stripping process for CO2 capture. Chem. Eng. J. 283, 1033–1043. https://doi.org/10.1016/j.cej.2015.08.086

Ma'mun, S., Nilsen, R., Svendsen, H.F., 2005. Solubility of Carbon Dioxide in 30 mass% Monoethanolamine and 50 mass% Methyldiethanolamine Solutions. J. Chem. Eng. Data 50, 630–634. https://doi.org/10.1021/je0496490

Ma'mun, S., Svendsen, H.F., Hoff, K.A., Juliussen, O., 2007. Selection of new absorbents for carbon dioxide capture. Energy Convers. Manag. 48, 251–258. https://doi.org/10.1016/j.enconman.2006.04.007

Mathias, P.M., O'Connell, J.P., 2012. The Gibbs-Helmholtz equation and the thermodynamic consistency of chemical absorption data. Ind. Eng. Chem. Res. 51, 5090–5097. https://doi.org/10.1021/ie202668k

Mathonat, C., Majer, V., Mather, A.E., Grolier, J.P.E., 1998. Use of flow calorimetry for determining enthalpies of absorption and the solubility of CO2 in aqueous monoethanolamine solutions. Ind. Eng. Chem. Res. 37, 4136–4141. https://doi.org/10.1021/ie9707679

Murrieta-Guevara, F., Rebolledo-Libreros, E., Trejo, A., 1992. Solubility of Carbon Dioxide in Binary Mixtures of N-Methylpyrrolidone with Alkanolamines. J. Chem. Eng. Data 37, 4–7. https://doi.org/10.1021/je00005a002

Oexmann, J., Kather, A., 2010. Minimising the regeneration heat duty of post-combustion CO2 capture by wet chemical absorption: The misguided focus on low heat of absorption solvents. Int. J. Greenh. Gas Control 4, 36–43. https://doi.org/10.1016/j.ijggc.2009.09.010

Oh, H., Ju, Y., Chung, K., Lee, C., 2020. Techno-economic analysis of advanced stripper configurations for post-combustion CO2 capture amine processes. Energy 206, 118164. https://doi.org/10.1016/j.energy.2020.118164

Pearson, P., Cousins, A., 2016. 18 - Assessment of corrosion inamine-based post-combustion capture of carbon dioxide systems, in: Absorption-Based Post-Combustion Capture of Carbon Dioxide. pp. 439–463. https://doi.org/10.1016/B978-0-08-100514-9.00018-4

Puxty, G., Maeder, M., 2016. Ch.2 - The fundamentals of post-combustion capture, Absorption-Based Post-combustion Capture of Carbon Dioxide. Elsevier Ltd., pp. 13-33. https://doi.org/10.1016/B978-0-08-100514-9.00002-0

Puxty, G., Rowland, R., Attalla, M., 2010. Comparison of the rate of CO2 absorption into aqueous ammonia and monoethanolamine. Chem. Eng. Sci. 65, 915–922. https://doi.org/10.1016/j.ces.2009.09.042

Raynal, L., Alix, P., Bouillon, P., Gomez, A., Nailly, D., Jacquin, M., Kittel, J., Mougin, P., Trapy, J., 2011. The DMX ™ process: an original solution for lowering the cost of post-combustion carbon capture. Energy Procedia 4, 779–786. https://doi.org/10.1016/j.egypro.2011.01.119

Raynal, L., Briot, P., Dreillard, M., Broutin, P., Salghetti, B., Politi, M., La, C., Thielens, M., Laborie, G., Normand, L., 2014. Evaluation of the DMX process for industrial pilot demonstration – methodology and results. Energy Procedia 63, 6298–6309.

https://doi.org/10.1016/j.egypro.2014.11.662

Ritchie, H., 2020. Overview of Global Energy [WWW Document]. Our World Data. URL https://ourworldindata.org/energy#more-than-80-of-our-energy-still-comes-from-fossil-fuels (accessed 2.24.21).

Ritchie, H., Roser, M., 2020. Greenhouse gas emissions [WWW Document]. Our World Data. URL https://ourworldindata.org/greenhouse-gas-emissions (accessed 2.17.21).

Rochelle, G.T., 2016. Ch.3 - Conventional amine scrubbing for CO2 capture, in: Absorption-Based Post-Combustion Capture of Carbon Dioxide. Elsevier Ltd., pp. 36–67. https://doi.org/10.1016/B978-0-08-100514-9.00003-2

Rochelle, G.T., 2009. Amine Scrubbing for CO_2 Capture. Science. 325, 1652–1654.

Rogelj, J., Shindell, D., Jiang, K., Fifita, S., Forster, P., Ginzburg, V., Handa, C., Kheshgi, H., Kobayashi, S., Kriegler, E., Mundaca, L., Séférian, R., Vilariño, M.V., 2018. Mitigation Pathways Compatible with 1.5°C in the Context of Sustainable Development, Global Warming of 1.5°C. An IPCC Special Report on the impacts of global warming of 1.5°C above pre-industrial levels and related global greenhouse gas emission pathways, in the context of strengthening the global response to the threat of climate change,. In Press.

Roussanaly, S., Jakobsen, J.P., Hognes, E.H., Brunsvold, A.L., 2013. Benchmarking of CO2 transport technologies: Part I-Onshore pipeline and shipping between two onshore areas. Int. J. Greenh. Gas Control 19, 584–594. https://doi.org/10.1016/j.ijggc.2013.05.031

Saha, A.K., Bandyopadhyay, S.S., Biswas, A.K., 1995. Kinetics of absorption of CO2 into aqueous solutions of 2-amino-2-methyl-1-propanol. Chem. Eng. Sci. 50, 3587–3598. https://doi.org/10.1016/0009-2509(95)00187-A

Sanku, M., Svensson, H., 2017. Crystallization Kinetics of AMP Carbamate in Solutions of AMP in Organic Solvents NMP or TEGDME. Energy Procedia 114, 840–851. https://doi.org/10.1016/j.egypro.2017.03.1226

Sanku, M.G., Svensson, H., 2020. Crystallization kinetics and the role of equilibrium in carbon capture systems with gas-liquid-solid equilibrium: Case study of AMP in NMP solution. Fluid Phase Equilib. 511, 112505. https://doi.org/10.1016/j.fluid.2020.112505

Sanku, M.G., Svensson, H., 2019. Modelling the precipitating non-aqueous CO2 capture system AMP-NMP, using the unsymmetric electrolyte NRTL. Int. J. Greenh. Gas Control 89, 20–32. https://doi.org/10.1016/j.ijggc.2019.07.006

Shen, K., Li, M., 1992. Solubility of Carbon Dioxide in Aqueous Mixtures of Monoethanolamine with Methyldiethanolamine. J. Chem. Eng. Data 37, 96–100. https://doi.org/10.1021/je00005a025

Shen, S., Bian, Y., Zhao, Y., 2017. Energy-efficient CO2 capture using potassium prolinate/ethanol solution as a phase-changing absorbent. Int. J. Greenh. Gas Control 56, 1–11. https://doi.org/10.1016/j.ijggc.2016.11.011

Sigma-Aldrich, 2021. Säkerhetsdatablad: N-metyl-2-pyrrolidon [WWW Document]. version 6.10. URL https://www.sigmaaldrich.com/SE/en/product/sial/328634?context=product (accessed 9.7.21).

Skagestad, R., Sundqvist, M., Biermann, M., 2017. Cutting Cost of CO2 Capture in Process Industry (CO2stCap) Project overview & first results for partial CO2 capture at integrated steelworks [WWW Document]. URL https://www.slideshare.net/globalccs/cutting-cost-of-co2-capture-in-process-%0Aindustry-co2stcap-project-overview-first-results-for-partial-co2-capture-at-integrated-steelworks (accessed 8.10.21).

Smith, K.H., Harkin, T., Mumford, K., Kentish, S., Qader, A., Anderson, C., Hooper, B., Stevens, G.W., 2017. Outcomes from pilot plant trials of precipitating potassium carbonate solvent absorption for CO2 capture from a brown coal fired power station in Australia. Fuel Process. Technol. 155, 252–260.

Song, C., Pan, W., Srimat, S.T., Zheng, J., Li, Y., Wang, Y.H., Xu, B.Q., Zhu, Q.M., 2004. Tri-reforming of methane over Ni catalysts for CO2 conversion to Syngas with desired H2/CO ratios using flue gas of power plants without CO2 separation. Stud. Surf. Sci. Catal. 153, 315–322. https://doi.org/10.1016/s0167-2991(04)80270-2

Svensson, H., Edfeldt, J., Zejnullahu Velasco, V., Hulteberg, C., Karlsson, H.T., 2014a. Solubility of carbon dioxide in mixtures of 2-amino-2-methyl-1-propanol and organic solvents. Int. J. Greenh. Gas Control 27, 247–254. https://doi.org/10.1016/j.ijggc.2014.06.004

Svensson, H., Hulteberg, C., Karlsson, H.T., 2014b. Precipitation of AMP carbamate in CO2 absorption process. Energy Procedia 63, 750–757. https://doi.org/10.1016/j.egypro.2014.11.083

Svensson, H., Karlsson, H.K., 2018. Solubility of carbon dioxide in mixtures of 2-amino-2-methyl-1-propanol and N-methyl2-pyrrolidone at absorption and desorption conditions, in: 14th Greenhouse Gas Control Technologies Conference Melbourne 21-26 October 2018 (GHGT-14). SSRN, pp. 1–8.

Svensson, H., Zejnullahu Velasco, V., Hulteberg, C., Karlsson, H.T., 2014c. Heat of absorption of carbon dioxide in mixtures of 2-amino-2-methyl-1-propanol and organic solvents. Int. J. Greenh. Gas Control 30, 1–8. https://doi.org/10.1016/j.ijggc.2014.08.022

Tong, D., Trusler, J.P.M., Maitland, G.C., Gibbins, J., Fennell, P.S., 2012. Solubility of carbon dioxide in aqueous solution of monoethanolamine or 2-amino-2-methyl-1-propanol: Experimental measurements and modelling. Int. J. Greenh. Gas Control 6, 37–47. https://doi.org/10.1016/j.ijggc.2011.11.005

United Nations Framework Convention on Climate Change, 2015. The Paris Agreement [WWW Document]. URL https://unfccc.int/process-and-meetings/the-paris-agreement/the-paris-agreement (accessed 7.29.21).

Vaidya, P.D., Kenig, E.Y., 2007. CO2-alkanolamine reaction kinetics: A review of recent studies. Chem. Eng. Technol. 30, 1467–1474. https://doi.org/10.1002/ceat.200700268

Versteeg, G.F., Van Dijck, L.A.J., Swaaij, W.P.M., 1996. On the kinetics between CO2 and alkanolamines both in aqueous and non-aqueous solutions. An overview. Chem. Eng. Comm. 144, 113–158.

Vitillo, J.G., Smit, B., Gagliardi, L., 2017. Introduction: Carbon Capture and Separation. Chem. Rev 117, 9521–9523. https://doi.org/10.1021/acs.chemrev.7b00403

Wanderley, R.R., Knuutila, H.K., 2020. Mapping Diluents for Water-Lean Solvents: A Parametric Study. Ind. Eng. Chem. Res. 59, 11656–11680. https://doi.org/10.1021/acs.iecr.0c00940

Wanderley, R.R., Pinto, D.D.D., Knuutila, H.K., 2020a. Investigating opportunities for water-lean solvents in CO2 capture: VLE and heat of absorption in water-lean solvents containing MEA. Sep. Purif. Technol. 231, 115883. https://doi.org/10.1016/j.seppur.2019.115883

Wanderley, R.R., Ponce, G.J.C., Knuutila, H.K., 2020b. Solubility and Heat of Absorption of CO2 into Diisopropylamine and N, N-Diethylethanolamine Mixed with Organic Solvents. Energy and Fuels 34, 8552–8561. https://doi.org/10.1021/acs.energyfuels.0c00880

Wanderley, R.R., Yuan, Y., Rochelle, G.T., Knuutila, H.K., 2019. CO2 solubility and mass transfer in water-lean solvents. Chem. Eng. Sci. 202, 403–416. https://doi.org/10.1016/j.ces.2019.03.052

Wang, T., Yu, W., Le, Y., Liu, F., Xiong, Y., He, H., Lu, J., Hsu, E., Fang, M., Luo, Z., 2017. Solvent regeneration by novel direct non-aqueous gas stripping process for post-combustion CO 2 capture 205, 23–32. https://doi.org/10.1016/j.apenergy.2017.07.040

Yuan, Y., Rochelle, G.T., 2018. CO2 absorption rate in semi-aqueous monoethanolamine. Chem. Eng. Sci. 182, 56–66. https://doi.org/10.1016/j.ces.2018.02.026

Zheng, C., Tan, J., Wang, Y.J., Luo, G.S., 2013. CO2 Solubility in a Mixture Absorption System of 2-Amino-2-methyl-1-propanol with Ethylene Glycol. Ind. Eng. Chem. Res. 52, 12247–12252. https://doi.org/10.1021/ie401805n

Zheng, C., Tan, J., Wang, Y.J., Luo, G.S., 2012. CO2 solubility in a mixture absorption system of 2-amino-2-methyl-1-propanol with glycol. Ind. Eng. Chem. Res. 51, 11236–11244. https://doi.org/10.1021/ie3007165